Chiral Nonet Mixing in $\eta' \to \eta\pi\pi$ Decay

Amir H. Fariborz, [a] *, Joseph Schechter [b] †, Soodeh Zarepour [c] ‡, and Mohammad Zebarjad [c] §
[a] *Department of Engineering, Science and Mathematics, State University of New York, Institute of Technology,Utica, NY13504-3050, USA,*
[b] *Department of Physics, Syracuse University, Syracuse, NY 13244-1130, USA, and*
[c] *Department of Physics, Shiraz University, Shiraz 71454, Iran*
(Dated: July 16, 2014)

Underlying mixing of scalar mesons is studied in $\eta' \to \eta\pi\pi$ decay within a generalized linear sigma model of low-energy QCD which contains two nonets of scalar mesons and two nonets of pseudoscalar mesons (a quark-antiquark nonet and a four quark nonet). The model has been previously employed in various investigations of the underlying mixings among scalar mesons below and above 1 GeV (as well as those of their pseudoscalar chiral partners) and has provided a coherent global picture for the physical properties and quark substructure of these states. The potential of the model is defined in terms of two- and four-quark chiral nonets, and based on the number of underlying quark and antiquark lines in each term in the potential, a criterion for limiting the number of terms at each order of calculation (and systematically further improving the results thereafter). At the leading order, which corresponds to neglecting terms in the potential with higher than eight quark and antiquark lines, the free parameters of the model have been previously fixed in detailed global fits to scalar and pseudoscalar experimental mass spectra below and above 1 GeV together with several low-energy parameters. In the present work, the same order of potential with fixed parameters is used to further explore the underlying mixings among scalar mesons in the $\eta' \to \eta\pi\pi$ decay. It is found that the linear sigma model with only a single lowest-lying nonet is not accurate in predicting the decay width, but inclusion of the mixing of this nonet with the next-to-lowest lying nonet, together with the effect of final state interaction of pions, significantly improves this prediction and agrees with experiment up to about 1%. It is also shown that while the prediction of the leading order of the generalized model for the Dalitz parameters is not close to the experiment, the model is able to give a reasonable prediction of the energy dependencies of the normalized decay amplitude squared and that this is expected to improve with further refinement of the complicated underlying mixings. Overall this investigation provides further support for the global picture of scalar mesons: those below 1 GeV are predominantly four-quark states and significantly mix with those above 1 GeV which are closer to the conventional p-wave quark-antiquark states.

PACS numbers: 14.80.Bn, 11.30.Rd, 12.39.Fe

arXiv:1407.3870v1 [hep-ph] 15 Jul 2014

I. INTRODUCTION

The scalar mesons continue to attract the attention of many investigators for their important roles in low-energy QCD [1]. Although not all their properties have been fully uncovered, nevertheless a great deal of progress has been made over the past couple of decades [2]-[70]. Now there seems to be an emerging agreement about their quark substructure. Historically, the light scalar mesons (below 1 GeV) with their low mass and inverted mass spectrum (isosinglet lighter than the isodoublet, lighter than the heavier isosinglet which is nearly degenerate in mass with isovector) found a natural template in an ideally mixed four-quark MIT bag model [71]. An ideally mixed pure four-quark picture, while gives a perfect description of the mass spectra of the scalars below 1 GeV, seems to need some distortions to be able to describe some of the decay channels of these states. On the other hand, the scalars above 1 GeV while seem to be close to the conventional p-wave quark-antiquark states, some of their properties deviate from such an idealized picture. In short, the scalars below 1 GeV appear to be close to four-quark states with some distortions and those above 1 GeV appear to be close to quark-antiquark states with some distortions. The natural question would be whether such distortions on the quark substructure of both of these sets of states is due to a mixing among these states. The idea of mixing is intuitively understandable since some of the scalars below and above 1 GeV are very broad (such as, for example, $f_0(500)$ and $f_0(1370)$, or $K_0^*(800)$) and there is no reason that they should

* Email: fariboa@sunyit.edu
† Email: schechte@phy.syr.edu
‡ Email: soodehzarepour@shirazu.ac.ir
§ Email: zebarjad@physics.susc.ac.ir

not refrain from mixing with members having the same quantum numbers in a nearby nonet (see refs. [72]-[78]). In [78], the idea of such mixings and their effects on the properties of isovectors and isodoublets was studied within a nonlinear chiral Lagrangian model and was shown that allowing a four-quark scalar nonet below 1 GeV to slightly mix with a quark-antiquark scalar nonet above 1 GeV provides a natural explanation for certain aspects of the mass spectrum and decay properties of both nonets of scalars. For example, it explains that when a pure four-quark nonet below 1 GeV mixes with a pure quark-antiquark nonet above 1 GeV, due to level repulsion, the scalar mesons below 1 GeV are pushed down in mass and hence become lighter than expected. Also it shows that several unexpected mass and decay properties of the scalars above 1 GeV stem from this underlying mixing: the fact that the experimental mass of $a_0(1450)$ is higher than that of $K_0^*(1430)$ (which is unexpected if these two states were to belong to the same pure quark-antiquark nonet) is due to a "level-crossing" that takes place in this mixing which also naturally explains several unexpected decay properties of the states above 1 GeV [78]. In refs. [79] (and refs. therein) such mixing patterns were further studied in a generalized linear sigma model. The advantages of linear vs nonlinear model are: (a) the scalar and pseudoscalar states become chiral partners, form chiral nonets, and the underlying chiral symmetry and its breakdown establishes connections and constrains on various parameters of the model (b) reliable experimental inputs on both scalar and pseudoscalar mesons can be used in determining the model parameters and (c) the status of some of the pseudoscalar states that are not quite established (such as $\eta(1405)$ which is stated to be a good "non-$\bar{q}q$" candidate [80], or dynamically generated in $f_0(980)\eta$ channel [81]) can be explored in this approach as well. The main disadvantage of linear model vs nonlinear model is the fact that in scattering and decay processes one has to carefully deal with the individual contributions that are often large but tend to regulate each other in a very delicate manner ("local cancelations"). This is a disadvantage compared to, for example, chiral perturbation theory [82] where corrections are systematically controlled at different orders. Nevertheless, for the present objective of studying the global picture for the family relations and mixings among various scalar states below 2 GeV, the generalized linear model in which all such states are explicitly kept in the Lagrangian, instead of being integrated out, seems to be an efficient framework. Although the description of $\eta' \to \eta\pi\pi$ seems to be beyond the immediate effectiveness of chiral perturbation theory [83], nevertheless, this decay has been studied in some variations of this framework [84].

The tree-level Feynman diagrams representing the $\eta' \to \eta\pi\pi$ decay are shown in Fig. 1. These include a four-point interaction diagram (contact diagram) together with diagrams representing the contributions of isovector and isosinglet scalar mesons. This is a suitable decay channel for studying the role of scalar mesons and their underlying mixing patterns. To probe the effect of such underlying mixings, we use both a single-nonet SU(3) linear sigma model, as well as a generalized version that contains two nonets of scalar mesons (a two-quark nonet and a four-quark nonet). In either case, the computation of the partial decay width, and the energy dependencies of the normalized decay amplitude, are the points of contact with experiment. The individual amplitudes are

$$\begin{aligned}
M_{4p} &= -\gamma^{(4)}, \\
M_{f_i} &= \sqrt{2}\gamma_{f_i\eta\eta'}\gamma_{f_i\pi\pi}\frac{1}{m_{f_i}^2+(p-k)^2} \\
&= \sqrt{2}\gamma_{f_i\eta\eta'}\gamma_{f_i\pi\pi}\frac{1}{m_{f_i}^2+\left[m_{\eta'}^2-m_\eta^2-2m_{\eta'}(w_1+w_2)\right]}, \\
M_{a_j} &= \gamma_{a_j\pi\eta'}\gamma_{a_j\pi\eta}\left[\frac{1}{m_{a_j}^2+(p-q_2)^2}+\frac{1}{m_{a_j}^2+(p-q_1)^2}\right] \\
&= \gamma_{a_j\pi\eta'}\gamma_{a_j\pi\eta}\left[\frac{1}{m_{a_j}^2+(-m_{\eta'}^2-m_\pi^2+2m_{\eta'}w_2)}+\frac{1}{m_{a_j}^2+(-m_{\eta'}^2-m_\pi^2+2m_{\eta'}w_1)}\right],
\end{aligned} \tag{1}$$

where the subscripts i and j run over the number of isosingle and isovector intermediate states, respectively, ω_1 and ω_2 are the pion energies, and the coupling constants are defined as

$$-\mathcal{L} = \frac{1}{2}\gamma^{(4)}\eta\eta'\boldsymbol{\pi}\cdot\boldsymbol{\pi}+\frac{\gamma_{f_i\pi\pi}}{\sqrt{2}}f_i\boldsymbol{\pi}\cdot\boldsymbol{\pi}+\gamma_{f_i\eta\eta}f_i\eta\eta+\gamma_{f_i\eta\eta'}f_i\eta\eta'+\gamma_{a_j\pi\eta}\mathbf{a_j}\cdot\boldsymbol{\pi}\eta+\gamma_{a_j\pi\eta'}\mathbf{a_j}\cdot\boldsymbol{\pi}\eta'+\cdots. \tag{2}$$

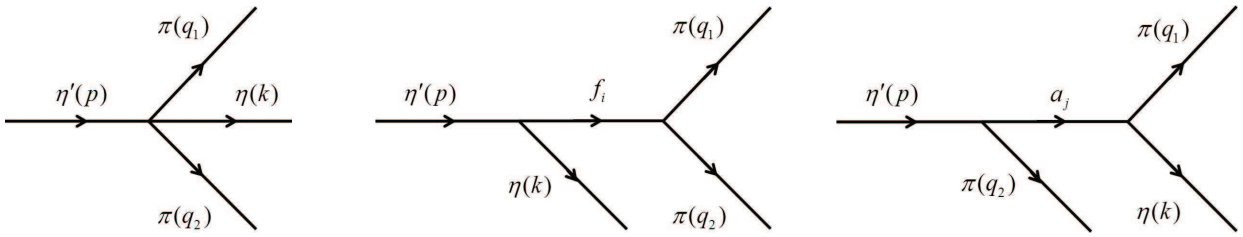

FIG. 1: Feynman diagrams representing the decay $\eta' \to \eta\pi\pi$: Contact term (left), contribution of isosinglet scalars (middle) and contribution of isovectors (right).

Following the standard calculation, the partial decay width is then obtained from

$$\Gamma_{\eta'\to\eta\pi\pi} = \frac{1}{64\pi^3 m_{\eta'}} \int dw_1 dw_2 |M|^2, \tag{3}$$

with the total amplitude

$$M = M_{4p} + \sum_i M_{f_i} + \sum_j M_{a_j}. \tag{4}$$

Equations (1), (2), (3) and (4) serve as our "templates" for various investigations in this work. The experimental data for decay width [1] is given in Table I.

TABLE I: Experimental decay width of $\eta' \to \eta\pi^+\pi^-$ (first column), $\eta' \to \eta\pi^0\pi^0$ (second column) and $\eta' \to \eta\pi\pi$ in the isospin invariant limit (last column).

	Exp. $[\eta' \to \eta\pi^+\pi^-]$	Exp. $[\eta' \to \eta\pi^0\pi^0]$	Exp. (averaged [a])
Γ (MeV)	0.086 ± 0.004	0.0430 ± 0.0022	0.086 ± 0.003

[a] For the average value $\bar{x} + \delta\bar{x}$ of measurements $x_i + \delta x_i$, we use $\bar{x} = \sum_i x_i w_i / \sum_i w_i; \delta\bar{x} = (\sum_i w_i)^{-1/2}$ with the weight $w_i = 1/(\delta x_i)^2$, and $\delta x_{\rm total} = \sqrt{\delta x^2_{\rm syst.} + \delta x^2_{\rm stat.}}$

In addition to the partial decay width, the energy dependence of the normalized decay amplitude squared can be compared with experiment. For this comparison, it is common to use Dalitz variables

$$\begin{aligned} X &= \frac{\sqrt{3}}{Q}(\omega_1 - \omega_2), \\ Y &= -\frac{2 + m_\eta/m_\pi}{Q}(\omega_1 + \omega_2) - 1 + \frac{2 + m_\eta/m_\pi}{Q}(m_{\eta'} - m_\eta), \end{aligned} \tag{5}$$

where $Q = m_{\eta'} - m_\eta - 2m_\pi$. Then the normalized decay amplitude squared can be expanded in powers of X and Y. In the generalized parametrization [1]

$$\mathcal{M}^2 = \frac{M(X,Y)^2}{M(0,0)^2} = 1 + a\,Y + b\,Y^2 + c\,X + d\,X^2 + \cdots, \tag{6}$$

where a, b, c, and d are real-valued parameters and $c = 0$ in the isospin invariant limit. The experimental data [1] for a, b and d are given in Table II. See also [87, 88].

TABLE II: Experimental Dalitz slope parameters for $\eta' \to \eta\pi^+\pi^-$ (first column), $\eta' \to \eta\pi^0\pi^0$ (second column) and $\eta' \to \eta\pi\pi$ in iso-spin invariant limit (third column).

Parameter	Exp. $[\eta' \to \eta\pi^+\pi^-]$	Exp. $[\eta' \to \eta\pi^0\pi^0]$	Exp. (averaged)
	VES [85]	GAM4[86]	iso-spin invariant limit
a	$-0.127 \pm 0.016 \pm 0.008$	$-0.066 \pm 0.016 \pm 0.003$	-0.094 ± 0.012
b	$-0.106 \pm 0.028 \pm 0.014$	$-0.063 \pm 0.028 \pm 0.004$	-0.082 ± 0.021
d	$-0.082 \pm 0.017 \pm 0.008$	$-0.067 \pm 0.020 \pm 0.003$	-0.075 ± 0.014

In Sec. II we present the predictions of single nonet SU(3) linear sigma model for the $\eta' \to \eta\pi\pi$ decay. We then present a brief review of the double nonet generalized linear sigma model in Sec. III, followed by its predictions for the relevant two-body decays in Sec. IV and of the $\eta' \to \eta\pi\pi$ decay in Sec. V. We give our approximation for the effect of final state interactions in Sec. VI and a summary and discussion of the results in Sec. VII.

II. SINGLE NONET APPROACH

The role of scalar mesons in $\pi\pi$, πK and $\pi\eta$ scattering channels was extensively studied in a single nonet SU(3) linear sigma model in [89]. It was shown that when the tree-level scattering amplitudes are unitarized with the simple K-matrix unitarization method, the model is able to explain the experimental data on the I=J=0 $\pi\pi$ scattering amplitude up to around 1.2 GeV. The first pole found in this unitarized amplitude clearly agrees with the properties of the light and broad sigma meson (with $m_\sigma = 0.457$ GeV and $\Gamma_\sigma = 0.632$ GeV), and the second pole agrees with the properties of $f_0(980)$ (with m_{f_0}=0.993 GeV and Γ_{f_0} =0.051 MeV). Within the same framework, a light and broad kappa meson (with m_κ=0.798-0.818 GeV and Γ_κ = 0.257-0.614 GeV) was identified in the studies of $I = 1/2$,$J = 0$, πK scattering amplitude. Similarly, a coherent picture was observed in the studies of $I = 1$, $J = 0$, $\pi\eta$ scattering amplitude in which a scalar resonance with the properties of $a_0(980)$ is clearly detected (with $m_{a_0} = 0.890$-1.013 GeV and Γ_{a_0}=0.109-0.241 GeV). These investigations were carried out within a non-renormalizable linear sigma model in which the Lagrangian has the general structure

$$\mathcal{L} = -\frac{1}{2}\mathrm{Tr}\left(\partial_\mu M \partial_\mu M^\dagger\right) - V_0\left(M\right) - V_{SB}, \tag{7}$$

where the chiral field M is constructed out of scalar nonet S and pseudoscalar nonet ϕ,

$$M = S + i\phi, \tag{8}$$

and transforms linearly under chiral transofrmation

$$M \to U_L M U_R^\dagger, \tag{9}$$

and V_0 is an arbitrary function of the independent $\mathrm{SU(3)_L}\times\mathrm{SU(3)_R}\times\mathrm{U(1)_V}$ invariants

$$\begin{aligned} I_1 &= \mathrm{Tr}\left(MM^\dagger\right), \qquad I_2 = \mathrm{Tr}\left(MM^\dagger MM^\dagger\right), \\ I_3 &= \mathrm{Tr}\left[\left(MM^\dagger\right)^3\right], \qquad I_4 = 6\left(\mathrm{det}M + \mathrm{det}M^\dagger\right). \end{aligned} \tag{10}$$

The symmetry breaker V_{SB} has the minimal form

$$V_{SB} = -2\mathrm{Tr}(AS), \tag{11}$$

where $A = \mathrm{diag}\,(A_1, A_2, A_3)$ are proportional to the three "current" type quark masses. The vacuum values satisfy

$$\langle S_a^b \rangle = \alpha_a \delta_a^b. \tag{12}$$

In the isospin invariant limit

$$A_1 = A_2 \neq A_3, \qquad \alpha_1 = \alpha_2 \neq \alpha_3. \tag{13}$$

Using "generating equations" that express the chiral symmetry of V_0 together with the minimum equation

$$\left\langle \frac{\partial V}{\partial S_a^b} \right\rangle = 0, \tag{14}$$

masses of pseudoscalars are completely determined based on the underlying chiral symmetry together with the choice of symmetry breakers (both $U(1)_A$ and $SU(3)_L \times SU(3)_R \to SU(2)$ isospin). The scalar masses on the other hand are not all predicted; in the most general case only the mass of isodoublet kappa meson is predicted, whereas if the renormalizability is imposed the isovector mass and one of the isosinglet masses are determined. It is found in [89] that it is necessary not to impose the renomalizability condition in order to be able to fit to the $\pi\pi$ and πK scatttering amplitudes and to get a reasonable description of $\pi\eta$ amplitude. In the nonrenormalizable case, the "bare" scalar masses $m_{BARE}(\sigma)$, $m_{BARE}(f_0)$ and $m_{BARE}(a_0)$ (i.e. the Lagrangian masses which are different than the physical masses that are related to the poles of the appropriate unitarized scattering amplitudes) and the scalar mixing angle θ_s are found from fits to various low-energy data in [89]. Here we use the same set of parameters to study the $\eta' \to \eta\pi\pi$ decay. In this case the required coupling constants in our "template" equations (1)-(4) are computed from the "generating equations" that express the symmetry of the Lagrangian (7) (a computational algorithm is presented in [90]):

$$\begin{aligned}
\gamma^{(4)} &= \sum_{a,b} \left\langle \frac{\partial^4 V}{\partial\phi_1^2 \partial\phi_2^1 \partial\phi_a^a \partial\phi_b^b} \right\rangle_0 (R_\phi)_2^a (R_\phi)_3^b, \\
\gamma_{a_0\pi\eta} &= \sum_{a} \left\langle \frac{\partial^3 V}{\partial S_1^2 \partial\phi_a^a \partial\phi_2^1} \right\rangle_0 (R_\phi)_2^a, \\
\gamma_{a_0\pi\eta'} &= \sum_{a} \left\langle \frac{\partial^3 V}{\partial S_1^2 \partial\phi_a^a \partial\phi_2^1} \right\rangle_0 (R_\phi)_3^a, \\
\gamma_{f_i\pi\pi} &= \frac{1}{\sqrt{2}} \sum_{a} \left\langle \frac{\partial^3 V}{\partial S_a^a \partial\phi_1^2 \partial\phi_2^1} \right\rangle_0 (R_s)_{i+1}^a, \\
\gamma_{f_i\eta\eta'} &= \sum_{a,b,c} \left\langle \frac{\partial^3 V}{\partial S_a^a \partial\phi_b^b \partial\phi_c^c} \right\rangle_0 (R_s)_{i+1}^a (R_\phi)_2^b (R_\phi)_3^c,
\end{aligned} \tag{15}$$

where the "bare" couplings and the rotation matrices (R_s and R_ϕ) are given in Appendix A. Here $f_1 = \sigma$ and $f_2 = f_0(980)$. We find

$$\Gamma(\eta' \to \eta\pi\pi) = 0.61 \pm 0.01\,\text{MeV} \qquad \text{Single nonet } (\textbf{bare}\,\text{result}). \tag{16}$$

Clearly, despite the success of the nonrenormalizable single nonet SU(3) linear sigma model in describing the low-energy scatterings discussed above, it estimates this partial decay width about seven times larger than the experimental value displayed in Table I.

The energy dependence of the normalized decay amplitude squared is compared with experiment in Fig. 2 and the Dalitz parameters that characterize the energy expansion of this amplitude squared are given in Table III. Comparing with the averaged experimental values of Table II, we see that there is a qualitative order of magnitude agreement, at best. This lack of accuracy of the single nonet approach raises the natural question of whether the underlying mixing among scalar mesons (which are clearly important players in this decay) has a noticeable effect on these estimates. One of the important roles of the scalars is to balance the large contribution due to the contact term (M_{4p}) as can be seen in Fig. 3. Moreover, the eta systems (both the two below 1 GeV as well as those above 1 GeV) can mix and have a nontrivial effect on this decay estimate. The single nonet approach does not take these mixing effects among the scalars and among the pseudoscalars into account which can have important consequences for this partial decay width. This motivates us to further study this decay within the generalized linear sigma model (that contains two scalar nonets and two pseudoscalar nonets) in this investigation.

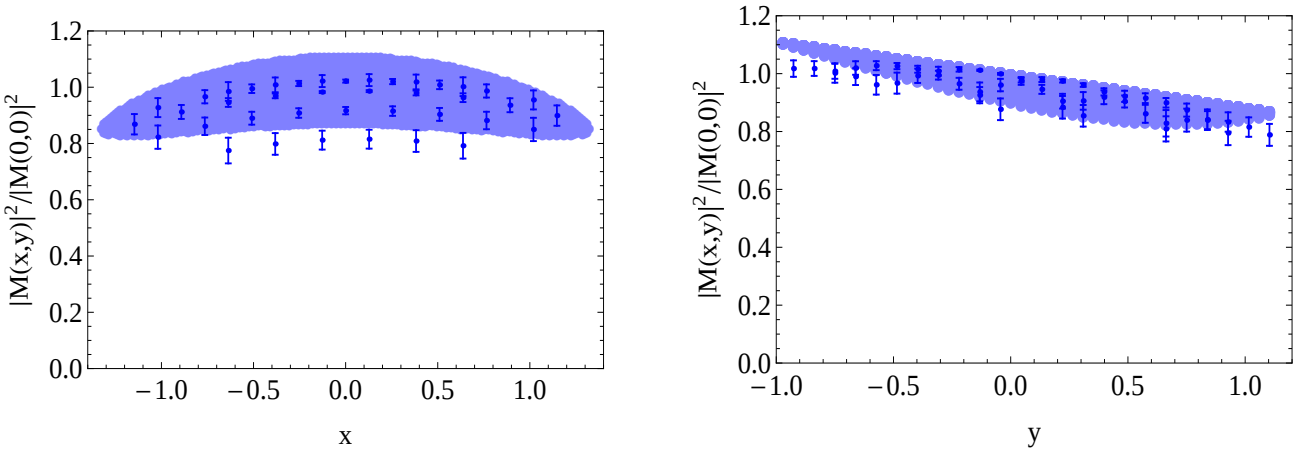

FIG. 2: Projections of $|\hat{M}|^2 = |M(x,y)|^2/|M(0,0)|^2$ onto the $y - |\hat{M}|^2$ and $x - |\hat{M}|^2$ planes (single nonet model).

TABLE III: The predicted Dalitz parameters in single nonet linear sigma model of ref. [89].

Parameter	single nonet model
a	-0.114 ± 0.001
b	-0.001 ± 0.001
d	-0.063 ± 0.001

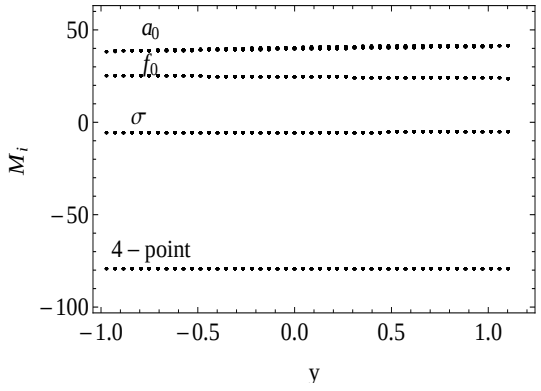

FIG. 3: Individual contributions to the $\eta' \to \eta\pi\pi$ decay amplitude in single nonet model. The large contribution of contact term M_{4p} is balanced with the contributions of $f_0(980)$ and $a_0(980)$.

III. BRIEF REVIEW OF THE GENERALIZED LINEAR SIGMA MODEL

The model employs the 3×3 matrix chiral nonet fields [79]:

$$M = S + i\phi, \qquad\qquad M' = S' + i\phi'. \tag{17}$$

The matrices M and M' transform in the same way under chiral SU(3) transformations but may be distinguished by their different $\mathrm{U}(1)_A$ transformation properties. M describes the "bare" quark-antiquark scalar and pseudoscalar nonet fields while M' describes "bare" scalar and pseudoscalar fields containing two quarks and two antiquarks. At the symmetry level in which we are working, it is unnecessary to further specify the four quark field configuration. The four quark field may, most generally, be imagined as some linear combination of a diquark-antidiquark and a "molecule" made of two quark-antiquark "atoms".

The general Lagrangian density which defines our model is

$$\mathcal{L} = -\frac{1}{2}\mathrm{Tr}\left(\partial_\mu M \partial_\mu M^\dagger\right) - \frac{1}{2}\mathrm{Tr}\left(\partial_\mu M' \partial_\mu M'^\dagger\right) - V_0\left(M, M'\right) - V_{SB}, \tag{18}$$

where $V_0(M, M')$ stands for a function made from $\mathrm{SU(3)_L}\times\ \mathrm{SU(3)_R}$ (but not necessarily $\mathrm{U(1)_A}$) invariants formed out of M and M'.

As previously discussed [79], the leading choice of terms corresponding to eight or fewer underlying quark plus antiquark lines at each effective vertex reads:

$$\begin{aligned} V_0 = \; & - \; c_2\,\mathrm{Tr}(MM^\dagger) + c_4^a\,\mathrm{Tr}(MM^\dagger MM^\dagger) \\ & + \; d_2\,\mathrm{Tr}(M'M'^\dagger) + e_3^a(\epsilon_{abc}\epsilon^{def} M_d^a M_e^b M_f'^c + h.c.) \\ & + \; c_3\left[\gamma_1 \ln(\frac{\det M}{\det M^\dagger}) + (1-\gamma_1)\ln\frac{\mathrm{Tr}(MM'^\dagger)}{\mathrm{Tr}(M'M^\dagger)}\right]^2. \end{aligned} \tag{19}$$

All the terms except the last two (which mock up the axial anomaly) have been chosen to also possess the $\mathrm{U(1)_A}$ invariance. A possible term $\left[\mathrm{Tr}(MM^\dagger)\right]^2$ is neglected for simplicity because it violates the OZI rule. The symmetry breaking term which models the QCD mass term takes the form given in Eq. (11). The model allows for two-quark condensates, $\alpha_a = \langle S_a^a \rangle$ as well as four-quark condensates $\beta_a = \langle S'^a_a \rangle$. Here we assume isotopic spin symmetry so $\mathrm{A_1}$ $=\mathrm{A_2} \neq \mathrm{A_3}$ and:

$$\alpha_1 = \alpha_2 \neq \alpha_3, \qquad\qquad \beta_1 = \beta_2 \neq \beta_3. \tag{20}$$

We also need the "minimum" conditions,

$$\left\langle \frac{\partial V_0}{\partial S} \right\rangle + \left\langle \frac{\partial V_{SB}}{\partial S} \right\rangle = 0, \qquad \left\langle \frac{\partial V_0}{\partial S'} \right\rangle = 0. \tag{21}$$

There are twelve parameters describing the Lagrangian and the vacuum: Six coupling constants given in Eq.(19), the two quark mass parameters, $(A_1 = A_2, A_3)$ and the four vacuum parameters $(\alpha_1 = \alpha_2, \alpha_3, \beta_1 = \beta_2, \beta_3)$. Ten of these parameters (c_2, c_4^a, d_2, e_3^a, α_1, α_3, β_1, β_3, A_1, A_3) are determined using the four minimum equations together with the following six experimental inputs for the masses, pion decay constant and the ratio of strange to non-strange quark masses:

$$\begin{aligned} m[a_0(980)] &= 984.7 \pm 1.2\,\mathrm{MeV}, \\ m[a_0(1450)] &= 1474 \pm 19\,\mathrm{MeV}, \\ m[\pi(1300)] &= 1300 \pm 100\,\mathrm{MeV}, \\ m_\pi &= 137\,\mathrm{MeV}, \\ F_\pi &= 131\,\mathrm{MeV}, \\ \frac{A_3}{A_1} &= 20 \to 30. \end{aligned} \tag{22}$$

Clearly, $m[\pi(1300)]$ and A_3/A_1 have large uncertainties which in turn dominate the uncertainty of predictions.

The remaining two parameters (c_3 and γ_1) only affect the isosinglet pseudoscalars (whose properties also depend on the ten parameters discussed above). However, there are several choices for determination of these two parameters depending on how the the four isosinglet pseudoscalars predicted in this model are matched to many experimental

candidates below 2 GeV. The two lightest predicted by the model (η_1 and η_2) are identified with $\eta(547)$ and $\eta'(958)$ with masses:

$$\begin{aligned} m^{\text{exp.}}[\eta(547)] &= 547.853 \pm 0.024\,\text{MeV}, \\ m^{\text{exp.}}[\eta'(958)] &= 957.78 \pm 0.06\,\text{MeV}. \end{aligned} \tag{23}$$

For the two heavier ones (η_3 and η_4), there are six ways that they can be identified with the four experimental candidates above 1 GeV: $\eta(1295)$, $\eta(1405)$, $\eta(1475)$, and $\eta(1760)$ with masses,

$$\begin{aligned} m^{\text{exp.}}[\eta(1295)] &= 1294 \pm 4\,\text{MeV}, \\ m^{\text{exp.}}[\eta(1405)] &= 1409.8 \pm 2.4\,\text{MeV}, \\ m^{\text{exp.}}[\eta(1475)] &= 1476 \pm 4\,\text{MeV}, \\ m^{\text{exp.}}[\eta(1760)] &= 1756 \pm 9\,\text{MeV}. \end{aligned} \tag{24}$$

This led to six scenarios considered in detail in [79]. The two experimental inputs for determination of the two parameters c_3 and γ_1 are taken to be $\text{Tr}M_\eta^2$ and $\det M_\eta^2$, i.e.

$$\begin{aligned} \text{Tr}\,\left(M_\eta^2\right) &= \text{Tr}\,\left(M_\eta^2\right)_{\text{exp}}, \\ \det\,\left(M_\eta^2\right) &= \det\,\left(M_\eta^2\right)_{\text{exp}}. \end{aligned} \tag{25}$$

Moreover, for each of the six scenarios, γ_1 is found from a quadratic equation, and as a result, there are altogether twelve possibilities for determination of γ_1 and c_3. Since only Tr and det of experimental masses are imposed for each of these twelve possibilities, the resulting γ_1 and c_3 do not necessarily recover the exact individual experimental masses, therefore the best overall agreement between the predicted masses (for each of the twelve possibilities) were examined in [79]. Quantitatively, the goodness of each solution was measured by the smallness of the following quantity:

$$\chi_{sl} = \sum_{k=1}^{4} \frac{\left|m_{sl}^{\text{theo.}}(\eta_k) - m_s^{\text{exp.}}(\eta_k)\right|}{m_s^{\text{exp.}}(\eta_k)}, \tag{26}$$

in which s corresponds to the scenario (i.e. $s = 1 \cdots 6$) and l corresponds to the solution number (i.e. $l =$ I, II). The quantity $\chi_{sl} \times 100$ gives the overall percent discrepancy between our theoretical prediction and experiment. For the six scenarios and the two solutions for each scenario, χ_{sl} was analyzed in ref. [79]. Some of these scenarios, such as those involving $\eta(1405)$ are clearly not favored. This suggests that $\eta(1405)$ is of a more complicated quark substructure that can be probed by the present model, and this is consistent with the investigation of ref. [81] in which it is shown that this state may be dynamically generated in $f_0(980)\eta$ interaction. For the third scenario (corresponding to identification of η_3 and η_4 with experimental candidates $\eta(1295)$ and $\eta(1760)$) and solution I the best agreement with the mass spectrum of the eta system was obtained (i.e. $\chi_{3\text{I}}$ was the smallest). For the present analysis too, all six scenarios are examined and it is again found that the best overall result (both for the partial decay width of $\eta' \to \eta\pi\pi$ as well as the energy dependence of its squared decay amplitude) is obtained for scenario "3I" consistent with the analysis of ref. [79]. In this work, we only present the result of "3I" scenario. To reduce the model uncertainty for the analysis of $\eta' \to \eta\pi\pi$ decay, we have further refined the numerical study of ref. [79] for scenario "3I" and have displayed the result in Fig. 4, in which $\chi_{3\text{I}}$ is plotted over the parameter space $m[\pi(1300)]$-A_3/A_1 that are two of the model inputs with largest experimental uncertainties.

Consequently, all twelve parameters of the model (at the present order of approximation) are evaluated by the method discussed above using four minimum equations and eight experimental inputs. The uncertainties of the experimental inputs result in uncertainties on the twelve model parameters which in turn result in uncertainties on physical quantities that are computed in this model. In the work of ref. [79] all rotation matrices describing the underlying mixing among two- and four-quark components for each spin and isospin states are computed. For scalars:

$$\begin{bmatrix} a_0^+(980) \\ a_0^+(1450) \end{bmatrix} = L_a^{-1} \begin{bmatrix} S_1^2 \\ S_1'^2 \end{bmatrix}, \qquad \begin{bmatrix} K_0(800) \\ K_0^*(1430) \end{bmatrix} = L_\kappa^{-1} \begin{bmatrix} S_1^3 \\ S_1'^3 \end{bmatrix}, \qquad \begin{bmatrix} f_1 \\ f_2 \\ f_3 \\ f_4 \end{bmatrix} = L_0^{-1} \begin{bmatrix} f_a \\ f_b \\ f_c \\ f_d \end{bmatrix}, \tag{27}$$

where L_a^{-1}, L_κ^{-1} and L_0^{-1} are the rotation matrices for $I = 1$, $I = 1/2$ and $I = 0$ respectively; $f_i, i = 1..4$ are four of the physical isosinglet scalars below 2 GeV (in this model f_1 and f_2 are clearly identified with $f_0(500)$ and $f_0(980)$

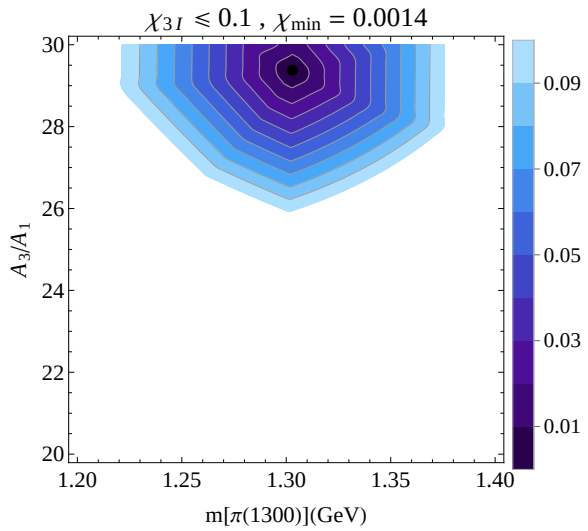

FIG. 4: Contour plot of function χ_{3I} [defined in Eq. (26)] over the $m[\pi(1300)]$-$A_3/A1$ plane for scenario "3I" in which the four isosinglet pseudoscalar states predicted by this model η_1, η_2, η_3 and η_4 are identified with the four experimental candidates $\eta(547)$, $\eta'(958)$, $\eta(1295)$ and $\eta(1760)$, respectively. The minimum of χ_{3I} occurs at $m[\pi(1300)] = 1.30$ GeV and A_3/A_1=29.40, at which it has a value of $\chi_{3I}^{\min} < 0.0015$, and shows an overall uncertainty of less than 0.15% between the four isosinglet pseudoscalar masses predicted by the model and the central values of the four experimental masses. (Note: the total experimental uncertainty $\sum_i \Delta m_i^{\text{exp.}}/m_i^{\text{exp.}} \approx 0.0083$ where $m_i^{\text{exp.}} \pm \Delta m_i^{\text{exp.}}, i = 1..4$ denote the four experimental masses.)

and the two heavier states resemble two of the heavier isosinglet scalars above 1 GeV); and

$$\begin{aligned} f_a &= \frac{S_1^1 + S_2^2}{\sqrt{2}} \qquad n\bar{n}, \\ f_b &= S_3^3 \qquad s\bar{s}, \\ f_c &= \frac{S_1'^1 + S_2'^2}{\sqrt{2}} \qquad ns\bar{n}\bar{s}, \\ f_d &= S_3'^3 \qquad nn\bar{n}\bar{n}. \end{aligned} \tag{28}$$

For pseudoscalars:

$$\begin{bmatrix} \pi^+(137) \\ \pi^+(1300) \end{bmatrix} = R_\pi^{-1} \begin{bmatrix} \phi_1^2 \\ \phi'^2_1 \end{bmatrix}, \qquad \begin{bmatrix} K^+(496) \\ K'^+(1460) \end{bmatrix} = R_K^{-1} \begin{bmatrix} \phi_1^3 \\ \phi'^3_1 \end{bmatrix}, \qquad \begin{bmatrix} \eta_1 \\ \eta_2 \\ \eta_3 \\ \eta_4 \end{bmatrix} = R_0^{-1} \begin{bmatrix} \eta_a \\ \eta_b \\ \eta_c \\ \eta_d \end{bmatrix}, \tag{29}$$

where R_π^{-1}, R_K^{-1} and R_0^{-1} are the rotation matrices for $I = 1$, $I = 1/2$ and $I = 0$ pseudoscalars respectively; $\eta_i, i = 1..4$ are four of the physical isosinglet pseudoscalars below 2 GeV; and

$$\begin{aligned} \eta_a &= \frac{\phi_1^1 + \phi_2^2}{\sqrt{2}} \qquad n\bar{n}, \\ \eta_b &= \phi_3^3 \qquad s\bar{s}, \\ \eta_c &= \frac{\phi'^1_1 + \phi'^2_2}{\sqrt{2}} \qquad ns\bar{n}\bar{s}, \\ \eta_d &= \phi'^3_3 \qquad nn\bar{n}\bar{n}. \end{aligned} \tag{30}$$

In the present work, we use the results obtained in [79] to compute the decay properties of $\eta' \to \eta\pi\pi$ without introducing any new parameters and find a reasonable agreement between the model prediction and experiment. This provides further test of the underlying two and four-quark mixing among scalar mesons below and above 1 GeV and the appropriateness of the generalized linear sigma model developed in [79] and reference therein.

IV. TWO BODY DECAYS

Since the scalar-pseudoscalar-pseudoscalar coupling constants are essential in analyzing the $\eta' \to \eta\pi\pi$ decay, for orientation we first calculate some of these couplings that appear in the prediction of the model for the main two-body decays of the scalar mesons below 1 GeV (for states above 1 GeV additional components such as mixing with glueballs would have to be included and will be presented in future works). The three decay widths that are particularly relevant for our analysis are,

$$\begin{aligned}
\Gamma[f_i \longrightarrow \pi\pi] &= 3\Big(\frac{q\,\gamma^2_{f_i\pi\pi}}{8\pi m^2_{f_i}}\Big) \\
\Gamma[a_j \longrightarrow \pi\eta] &= \frac{q\,\gamma^2_{a_j\pi\eta}}{8\pi m^2_{a_j}} \\
\Gamma[K_0^* \longrightarrow \pi K] &= 3\Big(\frac{q\,\gamma^2_{\kappa\pi K}}{16\pi m^2_{\kappa}}\Big)
\end{aligned} \tag{31}$$

where q is the center of mass momentum of the final state mesons (for a generic two-body decay $A \longrightarrow BC$ by $q = \sqrt{[m_A^2 - (m_B + m_C)^2][m_A^2 - (m_B - m_C)^2]}/(2m_A)$). The coupling constants are related to the bare couplings:

$$\begin{aligned}
\gamma_{f_i\pi\pi} &= \frac{1}{\sqrt{2}}\left\langle \frac{\partial^3 V}{\partial f_i\,\partial\pi^+\,\partial\pi^-}\right\rangle = \frac{1}{\sqrt{2}}\sum_{I,A,B}\left\langle \frac{\partial^3 V}{\partial f_I\,\partial(\phi_1^2)_A\,\partial(\phi_2^1)_B}\right\rangle (L_0)_{Ii}\,(R_\pi)_{A1}\,(R_\pi)_{B1}, \\
\gamma_{a\pi\eta} &= \left\langle \frac{\partial^3 V}{\partial a^-\,\partial\pi^+\,\partial\eta}\right\rangle = \sum_{A,B,I}\left\langle \frac{\partial^3 V}{\partial(S_1^2)_A\,\partial(\phi_1^2)_B\,\partial\eta_I}\right\rangle (L_a)_{A1}\,(R_\pi)_{B1}\,(R_0)_{I1}, \\
\gamma_{\kappa K\pi} &= \left\langle \frac{\partial^3 V}{\partial\kappa^0\,\partial K^-\,\partial\pi^+}\right\rangle = \sum_{A,B,C}\left\langle \frac{\partial^3 V}{\partial(S_2^3)_A\,\partial(\phi_3^1)_B\,\partial(\phi_1^2)_C}\right\rangle (L_\kappa)_{A1}\,(R_K)_{B1}\,(R_\pi)_{C1},
\end{aligned} \tag{32}$$

where A, B and C can take values of 1 and 2 (with 1 referring to nonet M and 2 referring to nonet M') and I is a placeholder for a,b,c and d that respectively represent the four bases in Eq. (28) and (30) . L_0, R_π, L_a, R_0, L_κ, R_K are the rotation matrices defined in previous Sec. III. The bare coupling constants are all given in Appendix A. The kappa coupling is defined as: $-\mathcal{L} = \frac{\gamma_{\kappa K\pi}}{\sqrt{2}}\left(\bar{K}\boldsymbol{\tau}\cdot\boldsymbol{\pi}\kappa + h.c.\right) + \cdots$.

We begin with the decay width of $f_0(500)$ to two pions which is the benchmark test of any low-energy QCD model. At the present level of approximation, the main uncertainties in fixing the free parameters of the model are on experimental inputs for the ratio of strange to nonstrange quark masses (A_3/A_2) and on the mass of $\pi(1300)$ resonance. Hence, the $m[\pi(1300)]$-A_3/A_1 plane is numerically scanned and the decay width is computed. The result is displayed in Fig. 5 showing that for most parts of the parameter space the lightest isosinglet state $f_0(500)$ (or σ) is broad with the decay width comparable to the latest PDG result. The decay width averaged over the entire parameter space is

$$\Gamma[f_0(500) \to \pi\pi] = 530 \pm 100\,\mathrm{MeV}, \tag{33}$$

where the uncertainty represents one standard deviation around the average. This is consistent with the decay width predicted in this model from the pole of the K-matrix unitatized $\pi\pi$ scattering amplitude. Therefore, the model clearly detects a light and broad isosinglet scalar meson.

Similarly, the prediction of the model over the $m[\pi(1300)]$-A_3/A_1 plane for $\Gamma[f_0(980) \to \pi\pi]$, $\Gamma[a_0(980) \to \pi\eta]$ and $\Gamma[K_0^*(800) \to \pi K]$ are shown in Fig. 5 with the averaged values:

$$\begin{aligned}
\Gamma[f_0(980) \to \pi\pi] &= 35 \pm 27\ \mathrm{MeV}, \\
\Gamma[a_0(980) \to \pi\eta] &= 57 \pm 44\ \mathrm{MeV}, \\
\Gamma[K_0^*(800) \to \pi K] &= 58 \pm 90\ \mathrm{MeV}.
\end{aligned} \tag{34}$$

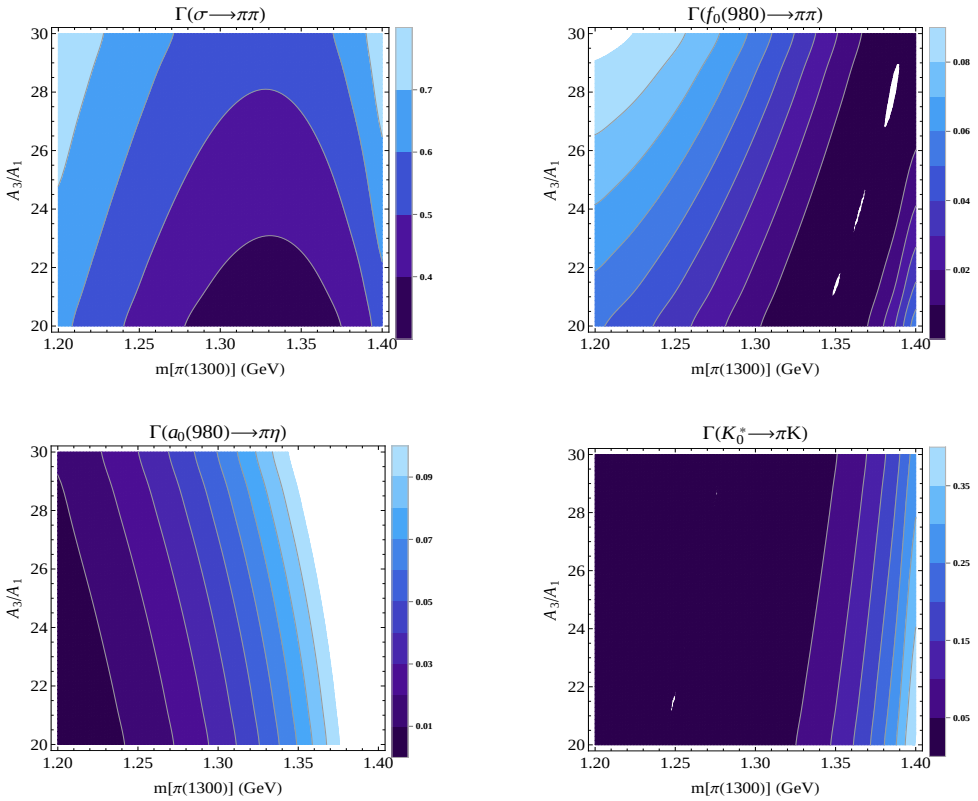

FIG. 5: Contour plots of the prediction of the model for the main two-body decay widths of light scalar mesons over the $m[\pi(1300)]$-A_3/A_1 plane: $\Gamma[f_0(500) \to \pi\pi]$ (top left) is predicted to be very large; $\Gamma[f_0(980) \to \pi\pi]$ (top right) and $\Gamma[a_0(980) \to \pi\eta]$ (bottom left) are within the expected experimental ranges; $\Gamma[K_0^*(800) \to \pi K]$ (bottom right) near high $m[\pi(1300)]$ mass is large, and in addition receives unitarity corrections due to the πK final-state interation.

The first three overlap with the expected experimental ranges [1]. The averaged decay width of $K_0^*(800)$ is not as large as expected, even though we see in Fig. 5 that there is a region in the parameter space (toward high values of $m[\pi(1300)]$) where this decay width has the right order of magnitude. However, in a separate work [93], it is shown that the prediction of the model for the $I = 1/2$, $J = 0$, πK scattering amplitude describes the experimental data well up to around 1 GeV. It is also shown that the poles of the K-matrix unitarized scattering amplitude (the κ pole) results in a light and broad $K_0^*(800)$ with a mass around 710-770 MeV and decay width around 610-700 MeV. We interpret the reduction in mass and the increase in the decay width to be the effect of the final state interactions of πK which are estimated by the simple K-matrix method.

The main two-body decay channels of the light scalars presented in this section are in a reasonable agreement with the experiment. This gives an initial test of some of the scalar-pseudoscalar-pseudoscalar coupling constants that will be incorporated in the study of $\eta' \to \pi\pi$ decay in the next section.

V. THE "BARE" PREDICTION OF THE GENERALIZED LINEAR SIGMA MODEL FOR $\eta' \to \eta\pi\pi$ DECAY

In this section we present the "bare" prediction of the model (i.e. without unitarity corrections due to the final state interaction of pions) for decay width and the energy dependencies of the normalized decay amplitude squared. In next Sec. we include the effect of these unitarity corrections. The Feynman diagrams of Fig. 1 include the contact term interaction together with the contributions of the four isosinglet scalars ($f_1, \cdots, f_4$) as well as the two isovector scalars (a_1 and a_2). Some of the scalar-pseudoscalar-pseudoscalar coupling constants were discussed in previous sections and the remaining ones are as follows:

$$\gamma^{(4)} = \sum_{I,J,A,B} \left\langle \frac{\partial^4 V}{\partial\eta_I \partial\eta_J \partial(\phi_1^2)_A \partial(\phi_2^1)_B} \right\rangle (R_0)_{I1}(R_0)_{J2}(R_\pi)_{A1}(R_\pi)_{B1},$$

$$\gamma_{f_i\eta\eta'} = \left\langle \frac{\partial^3 V}{\partial f_i \partial\eta\partial\eta'} \right\rangle = \sum_{K,I,J} \left\langle \frac{\partial^3 V}{\partial f_K \partial\eta_I \partial\eta_J} \right\rangle (L_0)_{Ki}(R_0)_{I1}(R_0)_{J2},$$

$$\gamma_{a_j\pi\eta'} = \left\langle \frac{\partial^3 V}{\partial a_j^+ \partial\pi^- \partial\eta'} \right\rangle = \sum_{A,B,I} \left\langle \frac{\partial^3 V}{\partial(S_1^2)_A \partial(\phi_2^1)_B \partial\eta_I} \right\rangle (L_a)_{Aj}(R_\pi)_{B1}(R_0)_{I2}, \quad (35)$$

where K, I,and J run over the bases a, b, c and d defined in Eqs. (28) and (30), and A and B can take values of 1, 2 (with 1 referring to nonet M and 2 to nonet $M^{'}$) and the rotation matrices are all defined in Eqs. (27) and (29). All "bare" coupling constants are calculated and presented in Appendix B.

We first note that the known "current algebra" result for this decay is recovered by decoupling the four-quark nonet M' and imposing the large scalar mass limit (see Appendix C). This illustrates how contributions of scalar mesons balance the large contribution of the four-point interaction and results in the known small "current algebra" result.

It is important to examine the "bare" predictions first in order to be able to then test different methods of unitarity corrections that in turn shed light on the important issue of final state interactions. Using the physical coupling constants defined above (together with those discussed in previous section) we compute the partial decay width by incorporating these couplings into our "template" equations (1)-(4). The "bare" predictions for scenario 3I (previously defined in Fig. 4) are plotted in Fig. 6 for the range of $m[\pi(1300)]$ and several values of A_3/A_1. Although the model prediction is of comparable order of magnitude to the experiment and gets closer to the experimental bounds for low values of $m[\pi(1300)]$, overall it is larger than that of experiment. The result is however closer to the experiment compared to that predicted by the single nonet approach. To find the best agreement we search for the values of $m[\pi(1300)]$ and A_3/A_1 that minimize function χ_Γ defined as

$$\chi_\Gamma(m[\pi(1300)], A_3/A_1) = \frac{|\Gamma^{\rm theo}(m[\pi(1300)], A_3/A_1) - \Gamma^{\rm exp.}|}{\Gamma^{\rm exp.}}. \quad (36)$$

We also use a χ^2 fit for doublecheck. The best predicted decay widths from χ and χ^2-fit are found with $m[\pi(1300)] = 1.22 \pm 0.01$ and $A_3/A_1 = 30.00 \pm 0.25$:

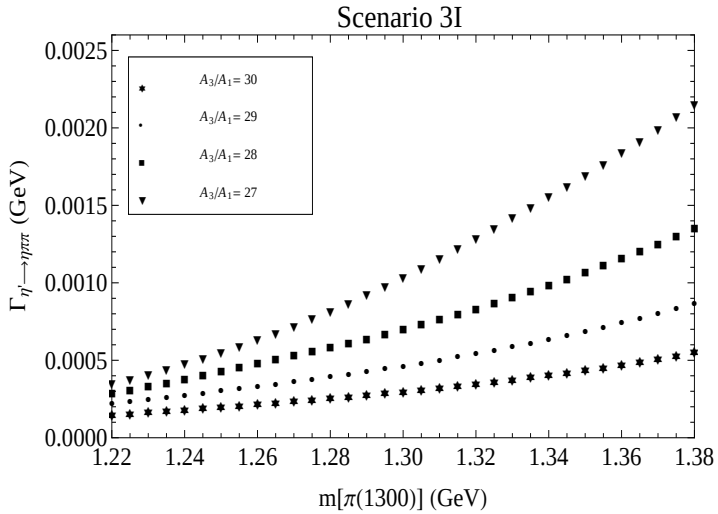

FIG. 6: "Bare" prediction (without unitarity corrections) of the generalized linear sigma model for partial decay width of $\eta' \to \eta\pi\pi$.

$$\Gamma(\eta' \to \eta\pi\pi) = 0.15 \pm 0.01\,\text{MeV} \qquad \text{Generalized linear sigma model (}\textbf{bare}\text{ result).} \quad (37)$$

The "bare" prediction for the energy dependence of the normalized decay amplitude squared is shown in Fig. 7 and compared with the averaged experimental data of Table II. The best fits to the Dalitz parameters result in best values of $m[\pi(1300)] = 1.38$ GeV and $A_3/A_1 = 28.75$ which are within the parameter space of the model [Eq. (22)] however do not coincide with the best values of these parameters found in the partial decay width analysis in Eq. (37). This shows that although inclusion of mixing among scalar and among pseudoscalars clearly improves the model predictions, nevertheless, it is necessary to account for the effect of final state interactions. A general characteristic of the linear sigma model is the cancelation of large four-point contribution with those of scalar mesons which for the "bare" predictions is shown in Fig. 8.

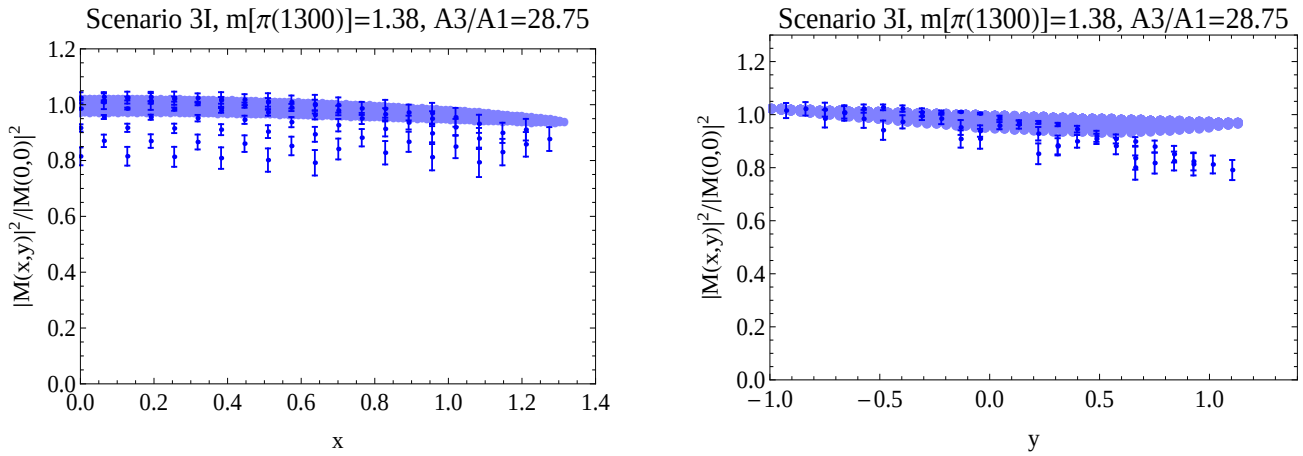

FIG. 7: Projections of $|\hat{M}|^2 = |M(x,y)|^2/|M(0,0)|^2$ onto the $y-|\hat{M}|^2$ and $x-|\hat{M}|^2$ planes ("bare" prediction of the generalized linear sigma model).

TABLE IV: Dalitz parameters obtained in fitting the "bare" generalized linear sigma model to experiment in a χ-fit [best point at $m[\pi(1300)] = 1.38\pm0.02$ and $A_3/A_1 = 28.75^{+1.25}_{-1.75}$] and a χ^2-fit [best point at $m[\pi(1300)] = 1.38\pm0.01$ and $A_3/A_1 = 27.25^{+1.50}_{-0.25}$].

Parameter	χ-fit	χ^2-fit
a	$-0.024^{+0.025}_{-0.017}$	$-0.039^{+0.015}_{-0.003}$
b	$0.0001^{+0.0110}_{-0.0034}$	$0.008^{+0.002}_{-0.008}$
d	$-0.029^{+0.012}_{-0.001}$	$-0.020^{+0.003}_{-0.009}$

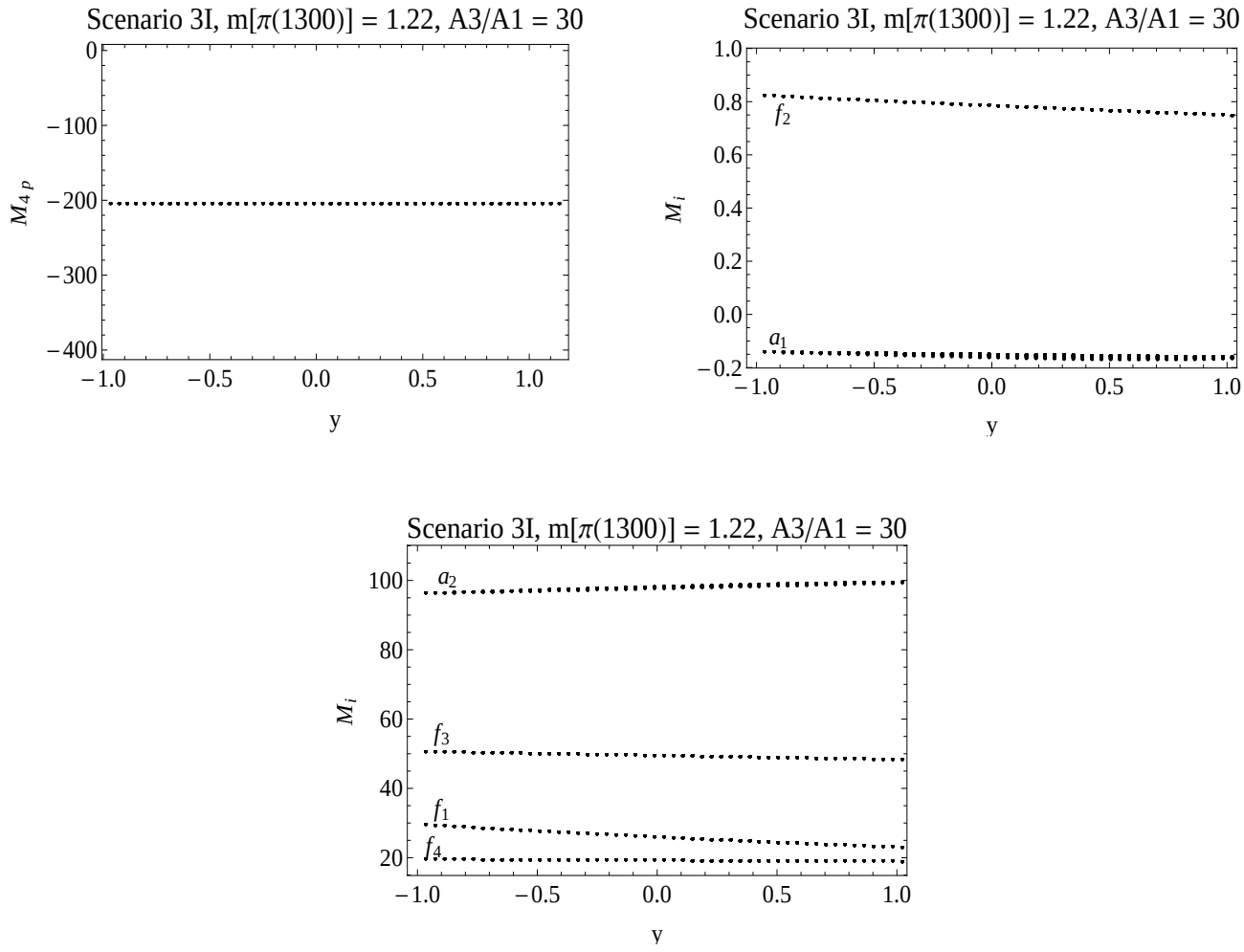

FIG. 8: Individual contributions to the "bare" decay amplitude of $\eta' \to \eta\pi\pi$. The large contribution of the contact terms is balanced with the large contributions of scalar mesons.

VI. UNITARITY CORRECTIONS

In principle there are corrections due to the final-state interactions of $\pi\pi$ and $\pi\eta$. These effects have been studied within the present model in ref. [92] in which the final-state interactions of pions were studied in unitarization of $\pi\pi$ scattering amplitude, and recently in unitarization of πK and $\pi\eta$ scattering amplitudes in [93, 94]. In the $\pi\pi$ analysis it is found that the effect of the final-state interactions on the properties of the sigma meson is large and this manifests itself in the substantial difference between the "bare" sigma mass (Lagrangian mass) and the physical sigma mass found from the pole of the K-matrix unitarized $I = J = 0$, $\pi\pi$ scattering amplitude (it is found [92] that the physical mass of sigma is around 480 MeV and its decay width is 450-500 MeV). On the contrary, the properties of $a_0(980)$ probed in the $\pi\eta$ scattering analysis [94] does not show a significant shift between the "bare" mass of $a_0(980)$ (Lagrangian mass) and that probed in the K-matrix unitarized $\pi\eta$ scattering amplitude. Since we are investigating the $\eta' \to \eta\pi\pi$ decay within the same framework of refs. [92, 94], we take the effect of $\pi\pi$ final state-interactions to be the dominant one.

Our main motivation in this work is to learn about the scalar meson mixing patterns, therefore, it is natural for us to approximate the unitarity corrections in a language that is explicitly expressed in terms of the shifts in the scalar mesons properties (from their "bare" Lagrangian values to their physical values). For this purpose, the K-matrix provides a reasonable tool to both account for unitarity corrections as well as to probe the underlying mixings. The

K-matrix has the advantage of not introducing any new parameters into the analysis, hence, allows establishing a direct connection between the "bare" Lagrangian properties of scalars and the physical properties of scalars probed in fits to appropriate experimental data. We follow the prior work presented in [92] in which a detailed analysis of $I = J = 0$, $\pi\pi$ scattering amplitude is given. The K-matrix unitarized scattering amplitude is given by

$$T_0^0 = \frac{{T_0^0}^B}{1 - i\,{T_0^0}^B}, \tag{38}$$

where ${T_0^0}^B$ is the "bare" scattering amplitude calculated from the Lagrangian. It is shown in [92] that

$${T_0^0}^B = T_\alpha + \sum_i \frac{T_\beta^i}{m_{f_i}^2 - s}, \tag{39}$$

with

$$\begin{aligned} T_\alpha &= \frac{1}{64\pi}\sqrt{1 - \frac{4m_\pi^2}{s}}\left[-5\,\gamma_{\pi\pi}^{(4)} + \frac{2}{p_\pi^2}\sum_i \gamma_{f_i\pi\pi}^2 \ln\left(1 + \frac{4p_\pi^2}{m_{f_i}^2}\right)\right], \\ T_\beta^i &= \frac{3}{16\pi}\sqrt{1 - \frac{4m_\pi^2}{s}}\,\gamma_{f_i\pi\pi}^2, \end{aligned} \tag{40}$$

where $p_\pi = \sqrt{s - 4m_\pi^2}/2$, the scalar-pseudoscalar-pseudoscalar couplings $\gamma_{f_i\pi\pi}$ are defined in Sec. I, and $\gamma_{\pi\pi}^{(4)}$ is the pion four-point coupling constant. It is shown in [89] that the K-matrix unitarized amplitude (38) can be expressed as a constant background and a sum over simple poles

$$T_0^0 \approx \tilde{T}_\alpha + \sum_i \frac{\tilde{T}_\beta^i}{z_i - s}, \tag{41}$$

where $\tilde{T}_\alpha$ is the constant (complex) background, the simple poles $z_i = \tilde{m}_i^2 - i\tilde{m}\tilde{\Gamma}_i$ with $\tilde{m}_i$ and $\tilde{\Gamma}_i$ being interpreted as the physical mass and decay width of the i-th isosinglet scalar meson, respectively, and $\tilde{T}_\beta^i$ are the residues. Moreover, it can be shown that

$$\left|\tilde{T}_\beta^i\right| \approx \tilde{m}_i\tilde{\Gamma}_i, \tag{42}$$

which resemble the corresponding numerators in "bare" amplitude (39) where

$$T_\beta^i\big|_{s=m_i^2} = m_i\Gamma_i. \tag{43}$$

Comparing (39), (41), (42) and (43) we see that unitarity corrections effectively shift the isosinglet scalar masses and decay widths

$$\begin{aligned} m_i &\to \tilde{m}_i \\ \Gamma_i &\to \tilde{\Gamma}_i \end{aligned} \tag{44}$$

In the decay $\eta' \to \eta\pi\pi$ the unitarity corrections for the sigma meson are the most important ones. We account for these corrections by shifting the "bare" mass and decay width to two pions according to (44). The second shift in (44) can also be expressed in terms of the shift in coupling constant, i.e.

$$\begin{aligned} m_\sigma &\to \tilde{m}_\sigma, \\ \gamma_{\sigma\pi\pi} &\to \tilde{\gamma}_{\sigma\pi\pi}, \end{aligned} \tag{45}$$

where $\tilde{m}_\sigma$ and $\tilde{\gamma}_{\sigma\pi\pi}$ are those found from the lowest pole $z_1 = \tilde{m}_\sigma^2 - i\tilde{m}_\sigma\Gamma_\sigma$ of the scattering amplitude [92] and since $\Gamma_\sigma \approx \Gamma[\sigma \to \pi\pi]$,

$$\tilde{\gamma}_{\sigma\pi\pi} = \sqrt{\frac{16\pi\tilde{m}_\sigma^2\Gamma_\sigma}{3\sqrt{\tilde{m}_\sigma^2 - 4m_\pi^2}}}. \tag{46}$$

Recalculating the partial decay width of $\eta' \to \eta\pi\pi$ (presented in the previous Sec.) with the new substitutions (45) we find the results displayed in Fig. 9, showing that the model predictions easily cross into the experimental range. The same effect can be taken into account for the $f_0(980)$, but that has a negligible effect on the results presented. On the two dimensional parameter space of the model ($m[\pi(1300)]$, A_3/A_1) the point that gives the best agreement with the experimental value of decay width is (1.29 GeV, 29.75) obtained by minimizing χ defined in Eq.(36) (as well as by minimizing the conventional χ^2). The decay width in this case is

$$\Gamma\left(\eta' \to \eta\pi\pi\right) = 0.085^{+0.003}_{-0.002}\,\text{MeV} \qquad \text{Generalized linear sigma model (}\textbf{unitarized}\text{ result).} \qquad (47)$$

This result is within 1.2% of experimental data on the decay width.

The energy dependencies of the normalized decay amplitude squared are plotted in Fig. 10, and fits to the Dalitz parameters are given in Table V. It is found that the point ($m[\pi(1300)]$, A_3/A_1) = (1.38 GeV, 29.75) gives the best agreement with the experiment. Although this point and the best point for the decay width (presented above) are both within the parameter space of the model, they do not coincide, showing the need for further improvement of this complicated decay and will be further discussed in next section. The general feature of linear sigma model in which scalar mesons "conspire" to balance the large contribution of the contact term can be seen in Fig. 11.

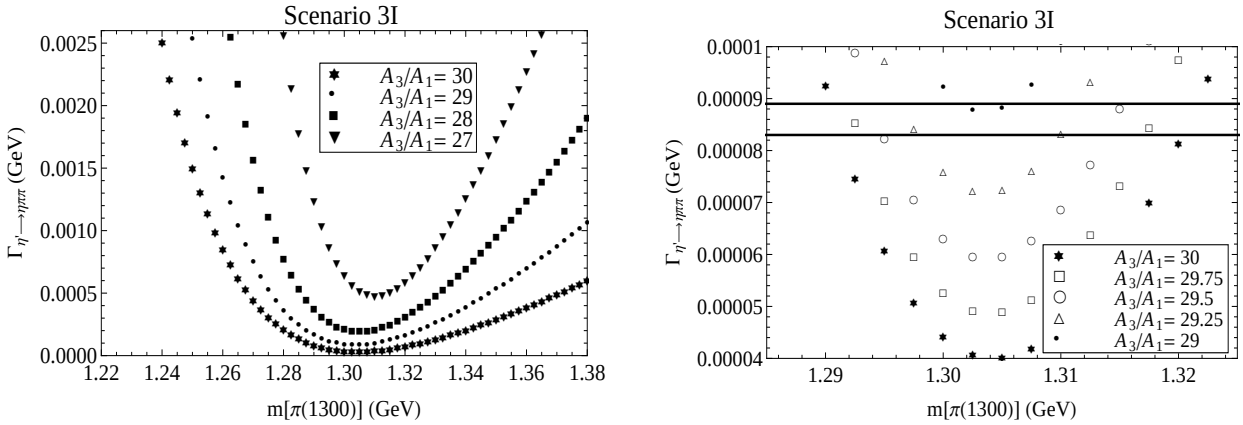

FIG. 9: Prediction of the generalized linear sigma model for the partial decay width of $\eta' \to \eta\pi\pi$. The final-state interactions of pions are taken into account by shifting the mass and coupling constant of sigma meson according to Eq. (45).

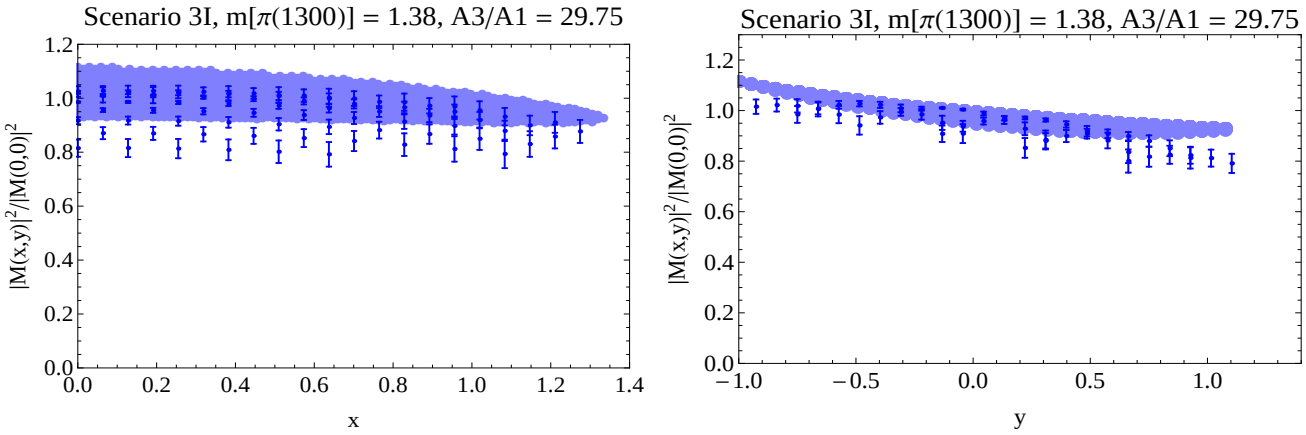

FIG. 10: Projects of the normalized decay amplitude squared onto planes containing x and y parameters (shaded regions) are compared with the experimental data (error bars). The final-state interactions of pions are taken into account by shifting the mass and coupling constant of sigma meson according to Eq. (45).

TABLE V: Dalitz parameters in unitarized generalized linear sigma model from fits (both χ-fit as well as χ^2 fit) to experiment. The presented results are the closest agreement with experiment that occur at point $(m[\pi(1300)],A_3/A_1)$ = (1.38±0.01 GeV, 29.75±0.25).

Parameter	χ-fit	χ^2-fit
a	$-0.079^{+0.019}_{-0.021}$	-0.079 ± 0.019
b	$0.024^{+0.010}_{-0.009}$	0.024 ± 0.009
d	-0.028 ± 0.001	-0.028 ± 0.001

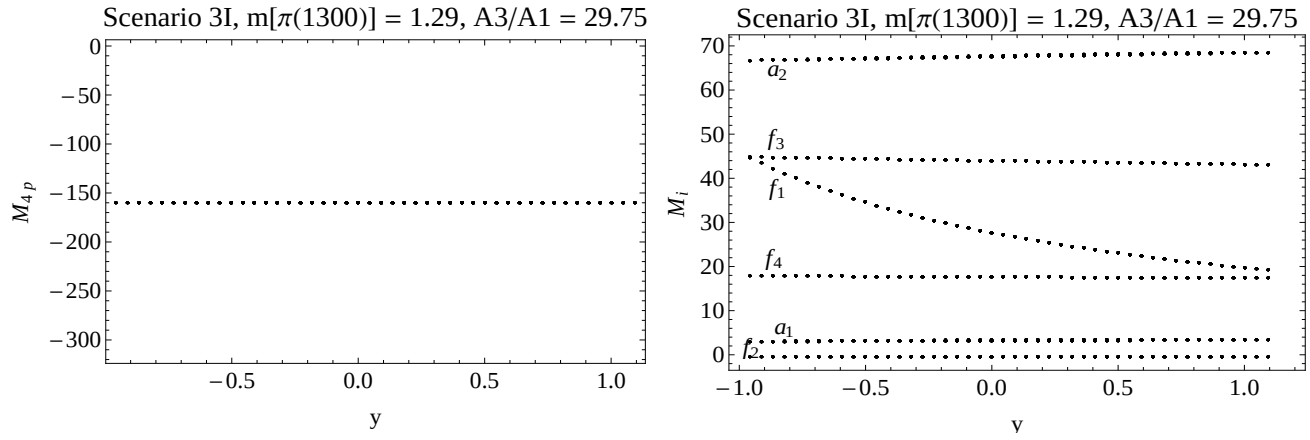

FIG. 11: Individual contributions to the decay amplitude. The final-state interactions of pions are taken into account by shifting the mass and coupling constant of sigma meson according to Eq. (45).

Similarly, we can estimate the final state interactions for the single nonet model of Sec. II. We find that the decay width improves

$$\Gamma\left(\eta' \to \eta\pi\pi\right) = 0.35 \pm 0.01 \text{ MeV} \qquad \text{Single nonet } (\textbf{unitarized} \text{ result}). \tag{48}$$

However, the energy dependencies worsen in this case (Fig. VI and Table VI). This shows that the effect of unitarity corrections alone are not sufficient and there seems to be the effect of mixing that should be taken into account.

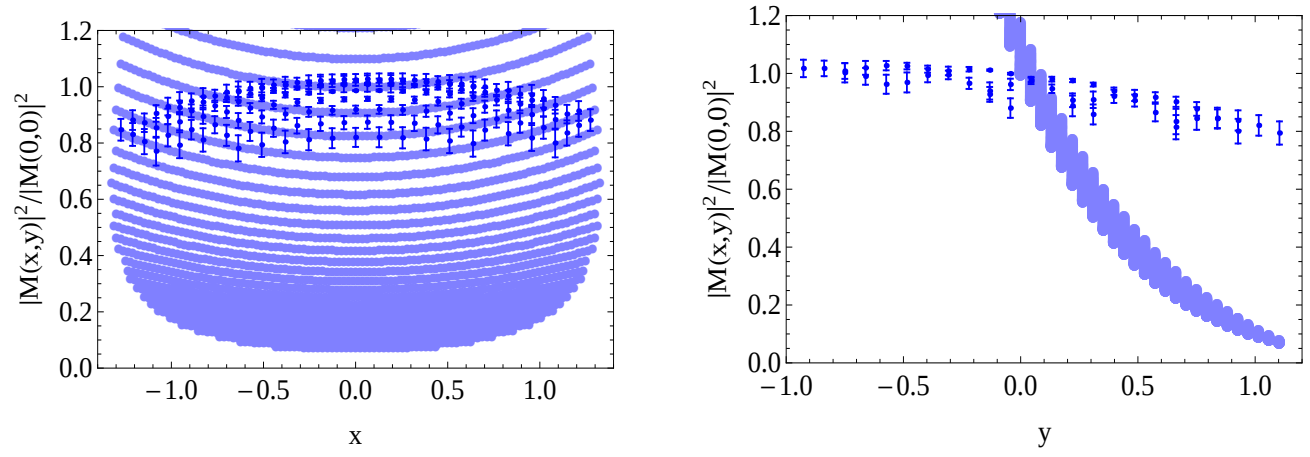

FIG. 12: Projections of $|\hat{M}|^2 = |M(x,y)|^2/|M(0,0)|^2$ onto the $y - |\hat{M}|^2$ and $x - |\hat{M}|^2$ planes (unitarized single nonet model). While the effect of final state interactions improves the partial decay width predicted by the single nonet model, the energy dependencies worsen. This shows that there is more into this decay that just the effect of final-state interactions.

TABLE VI: Predicted decay parameters in the unitarized single nonet approach of ref. [89].

Parameter	single nonet model
a	-2.17 ± 0.01
b	2.37 ± 0.01
d	0.11 ± 0.01

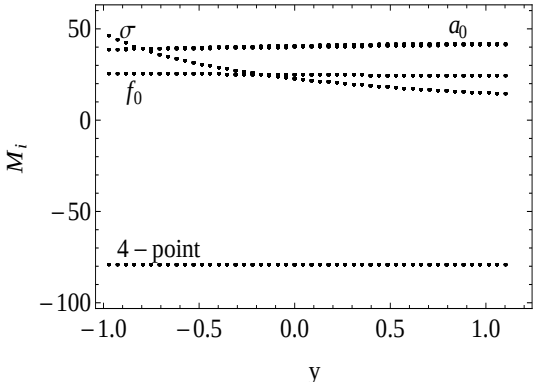

FIG. 13: Individual contributions to the $\eta' \to \eta\pi\pi$ decay amplitude in unitarized single nonet model. The large contribution of contact term M_{4p} is balanced with the contributions of scalars. Unitarity corrections are taken into account.

VII. CONCLUDING DISCUSSION

In this work, we examined the $\eta' \to \eta\pi\pi$ decay as a probe of scalar mesons substructure and mixing patterns within a generalized linear sigma model of low-energy QCD that is formulated in terms of two scalar meson nonets and two pseudoscalar meson nonets (a two- and a four-quark nonet for each spin). We first showed that the single nonet model of ref. [89], despite its considerable success in describing $\pi\pi$, πK and $\pi\eta$ low-energy scatterings, gives inaccurate predictions for the partial decay width of $\eta' \to \eta\pi\pi$ as well as the energy dependencies of its normalized decay amplitude squared. Since this decay involves η and η' as well as intermediate scalar mesons and that these states are known to have nontrivial mixings with states with the same quantum numbers above 1 GeV, and since such mixings have been previously [79] given important insights into the physical properties of both scalar as well as pseudoscalar mesons, in this work we explored the effect of these mixings on this decay. We investigated whether the inclusion of mixing can have a tangible effect and whether such effects improve the predictions of the single nonet linear sigma model for this decay. We showed that inclusion of the underlying mixings (even without unitarity corrections) considerably improves the partial decay width prediction as well as the energy dependencies of the normalized decay amplitude squared. We then showed that inclusion of the final state interaction of pions further improves the predictions and brings the partial decay width to within 1.2% of its experimental value, and considerably improves the predictions for the Dalitz parameters. Our findings are summarized in several tables in this final section. Table VII gives our results for the partial decay width and Dalitz parameters in single nonet linear sigma model as well as its generalized version, both with and without accounting for the final state interaction of pions.

We note that while the predictions of Dalitz parameters are improved in the fourth column of Table VII, they are still far from their experimental values. However, we further note that since the Dalitz variables X and Y are relatively small over much of their domain, the difference in the normalized decay amplitude itself is not that large for most of the domain. To illustrate this, Fig. 14 zooms in on the X, Y domain in four steps. Inside each "loop" the closeness of the model prediction for the energy dependence of the normalized decay amplitude squared is measured

with the quantity

$$\bar{\chi}_{\mathcal{M}^2} = \frac{1}{N}\sum_{i}^{N}\frac{\left|\left(\mathcal{M}^2\right)^{\text{exp.}}(X_i,Y_i) - \left(\mathcal{M}^2\right)^{\text{theo.}}(X_i,Y_i)\right|}{\left(\mathcal{M}^2\right)^{\text{exp.}}(X_i,Y_i)}, \tag{49}$$

where the normalized decay matrix element is defined in Eq.(6) and the averaged experimental data in Table II. The results are presented in Table VIII and clearly show an averaged agreement with experiment (for the two cases that the best energy dependencies are obtained is around 6%), despite the much less agreement on Dalitz coefficients displayed in Table VII.

The dependence of the results on the choice of points in the two dimensional parameter space $m[\pi(1300)]$ and A_3/A_1 are summarized in Tables IX and X. The fact that the best points for the partial decay width and energy dependencies of the normalized decay amplitude squared do not occur at the same point, can be interpreted as an estimate of our theoretical uncertainty. At the present order of accuracy of this model, we have ignored effects such as terms in the potential with higher than eight quark and antiquark lines as well as the scalar and pseudoscalar glueballs. Both of these are expected to have some effects on the results. Since the $\mathrm{U(1)_A}$ anomaly plays an important role in the eta sector, we have made an initial investigation of the effect of the higher order $\mathrm{U(1)_A}$ breaking term (which are related to higher order instanton contributions at the quark level) and have observed that this term improves the picture by bringing the two points in the parameter space closer together. This is quite encouraging and will be presented in detail in a separate work [95]. It is also interesting to further apply the present model to study the isospin violating $\eta \to 3\pi$ decay [96, 97], and to examine the effect of various unitarization methods [98].

TABLE VII: Comparing with experiment the predictions by the single nonet linear sigma model (first two columns) and those by the generalized linear sigma model (the last two columns) for the decay width and the Dalitz parameters of $\eta' \to \eta\pi\pi$ decay. The goodness of the predictions are measured by the smallness of the parameter χ defined for a generic quantity q as $\chi_q = \left|(q^{\text{exp.}} - q^{\text{theo.}})/q^{\text{exp.}}\right|$ (i.e. $\chi_q \times 100$ gives the percent difference between theory and experiment). The predictions of the generalized linear sigma model depend on the choice of points in its two dimensional parameter space ($m[\pi(1300)]$, A_3/A_1): In the third column, the minimum of χ_Γ and of $\chi_{\text{Dalitz}} = \chi_a + \chi_b + \chi_d$ occur at point (1.22 GeV, 30.00) and at point (1.38 GeV, 28.75), respectively, whereas in the fourth column, the minimum of χ_Γ and of χ_{Dalitz} occur at (1.29 GeV, 29.75) and at (1.38 GeV, 29.75), respectively. Clearly, the shortcomings of the single nonet linear sigma model of ref. [89] can be seen in the first two columns: the decay width is several times larger than the experimental value and the unitarity corrections do not improve the situation and in fact worsen the Dalitz parameter predictions. On the other hand, the generalized linear sigma model significantly improves the predictions and gives the decay width in the unitarized version to 1.2% of the experimental value and also improves the Dalitz parameter predictions.

	single nonet (Bare)	single nonet (Unitarized)	MM' (Bare)	MM' (Unitarized)
χ_Γ	6.09	3.07	0.74	0.012
χ_a	0.21	22.08	0.74	0.16
χ_b	0.99	30.02	1.0	1.29
χ_d	0.16	2.4	0.61	0.63
χ_{total}	7.45	57.57	3.10	2.09

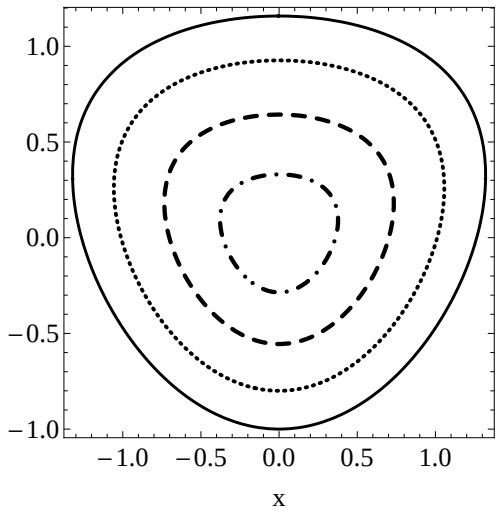

FIG. 14: The breakdown of XY domain into four subregions ("loops").

TABLE VIII: Displayed numbers in the second to last columns are $\bar{\chi}_{\mathcal{M}^2}$ [defined in Eq. (49)] over the four "loops" of Fig. 14 [see Eq.(6)]. The predictions of the generalized linear sigma model depend on the choice of points in its two dimensional parameter space ($m[\pi(1300)]$, A_3/A_1). The displayed values of $m[\pi(1300)]$ and A_3/A_1 give the best result for partial decay width without/with the final state interactions (first/third rows); and the best result for the energy dependencies of the normalized decay amplitude squared without/with the final-state interactions (second/fourth row).

$m[\pi(1300)]$(GeV)	A_3/A_1	Dotted-Dashed	Dashed	Dotted	Solid
1.22	30.00	0.14	0.27	0.41	0.54
1.38	28.75	0.01	0.03	0.04	0.07
1.29	29.75	1.0	2.2	4.7	7.6
1.38	29.75	0.005	0.02	0.04	0.06

TABLE IX: Dependency on the choices of $m[\pi(1300)]$, A_3/A_1 of the "bare" model predictions (without the effect of unitarity corrections due to the final state interaction of pions). In the first to last columns, respectively, the values of these two parameters are 1.30 GeV, 29.40 (best model prediction for the eta masses); 1.22 GeV, 30.00 (best prediction for the decay width) and 1.38 GeV, 28.75 (best prediction for the energy dependencies). In each column the targeted quantities are highlighted in bold and their closeness to experimental data is measured with their corresponding χ.

MM' (Bare)	$(\chi_{\rm min})_{\rm mass}$ = 0.14%	$(\chi_{\rm min})_{\Gamma}$ = 74%	$(\chi_{\rm min})_{\rm E.D.}$ = 235%
$m[\pi(1300)]$	1300	1220	1380
A_3/A_1	29.40	30.00	28.75
m_{η_1}(MeV)	**547**	554	539
m_{η_2}(MeV)	**959**	979	947
m_{η_3}(MeV)	**1294**	1229	1364
m_{η_4}(MeV)	**1756**	1788	1710
Γ(MeV)	0.42	**0.15**	0.97
a	0.24	0.88	**−0.024**
b	−0.026	0.07	**0.0001**
d	−0.037	−0.07	**−0.029**

TABLE X: Dependency on the choices of $m[\pi(1300)]$, A_3/A_1 of the "unitarized" model predictions (with the effect of the final state interaction of pions). In the first to last columns, respectively, the values of these two parameters are 1.3 GeV, 29.40 (best model prediction for the eta masses); 1.29 GeV, 29.75 (best prediction for the decay width) and 1.38 GeV, 29.75(best prediction for the energy dependencies). In each column the targeted quantities are highlighted in bold and their closeness to experimental data is measured with their corresponding χ.

MM' (Unitarized)	$(\chi_{\rm min})_{\rm mass}$ $= 0.14\%$	$(\chi_{\rm min})_{\Gamma}$ $= 1.2\%$	$(\chi_{\rm min})_{\rm E.D.}$ $= 207\%$
$m[\pi(1300)]$	1300	1290	1380
A_3/A_1	29.40	29.75	29.75
m_{η_1}(MeV)	**547**	550	544
m_{η_2}(MeV)	**959**	956	936
m_{η_3}(MeV)	**1294**	1285	1364
m_{η_4}(MeV)	**1756**	1762	1715
Γ(MeV)	0.072	**0.085**	0.62
a	10.84	-9.48	$\mathbf{-0.079}$
b	24.72	26.2	**0.024**
d	-0.29	0.22	$\mathbf{-0.028}$

Appendix A: Coupling constants in the single-nonet model

The rotation matrices are

$$\begin{bmatrix} \pi^0 \\ \eta \\ \eta' \end{bmatrix} = R_\phi(\theta_p) \begin{bmatrix} \phi_1^1 \\ \phi_2^2 \\ \phi_3^3 \end{bmatrix} = \begin{bmatrix} \frac{1}{\sqrt{2}} & -\frac{1}{\sqrt{2}} & 0 \\ \frac{a_p}{\sqrt{2}} & \frac{a_p}{\sqrt{2}} & -b_p \\ \frac{b_p}{\sqrt{2}} & \frac{b_p}{\sqrt{2}} & a_p \end{bmatrix} \begin{bmatrix} \phi_1^1 \\ \phi_2^2 \\ \phi_3^3 \end{bmatrix}, \tag{A1}$$

with $a_p = (\cos\theta_p - \sqrt{2}\sin\theta_p)/\sqrt{3}$, $b_p = (\sin\theta_p + \sqrt{2}\cos\theta_p)/\sqrt{3}$, where θ_p is the pseudoscalar (octet-singlet) mixing angle. Similarly,

$$\begin{bmatrix} a_0^0 \\ \sigma \\ f_0 \end{bmatrix} = R_s(\theta_s) \begin{bmatrix} S_1^1 \\ S_2^2 \\ S_3^3 \end{bmatrix} = \begin{bmatrix} \frac{1}{\sqrt{2}} & -\frac{1}{\sqrt{2}} & 0 \\ \frac{a_s}{\sqrt{2}} & \frac{a_s}{\sqrt{2}} & -b_s \\ \frac{b_s}{\sqrt{2}} & \frac{b_s}{\sqrt{2}} & a_s \end{bmatrix} \begin{bmatrix} S_1^1 \\ S_2^2 \\ S_3^3 \end{bmatrix}, \tag{A2}$$

with $a_s = (\cos\theta_s - \sqrt{2}\sin\theta_s)/\sqrt{3}$, $b_s = (\sin\theta_s + \sqrt{2}\cos\theta_s/\sqrt{3}$ where θ_s is the scalar (octet-singlet) mixing angle.

The coupling constants are:

$$\begin{aligned} \gamma^{(4)} = \quad & -\frac{1}{(2F_K - F_\pi)F_\pi^3} a_p b_p \Big[-4F_K^2 \Big(5\sqrt{2} a_p b_p (m_\eta^2 - m_{\eta'}^2) - 84 F_\pi V_4 \Big) \\ & + F_\pi^2 \Big(4 m_{\rm BARE}^2(a_0) + 2 m_{\rm BARE}^2(\sigma) a_s^2 + 2\sqrt{2}(m_{\rm BARE}^2(f_0) - m_{\rm BARE}^2(\sigma) a_s b_s \\ & + 2 m_{\rm BARE}^2(f_0) b_s^2 - 6 a_p^2 m_\eta^2 - 7\sqrt{2} a_p b_p m_\eta^2 + 7\sqrt{2} a_p b_p m_{\eta'}^2 - 6 b_p^2 m_{\eta'}^2 + 84 F_\pi V_4 \Big) \\ & - 4 F_K F_\pi \Big(2 m_{\rm BARE}^2(a_0) + m_{\rm BARE}^2(\sigma) a_s^2 + m_{\rm BARE}^2(f_0) b_s^2 - 3 a_p^2 m_\eta^2 - 5\sqrt{2} a_p b_p m_\eta^2 \\ & + 5\sqrt{2} a_p b_p m_{\eta'}^2 - 3 b_p^2 m_{\eta'}^2 + 84 F_\pi V_4 \Big) \Big], \end{aligned} \tag{A3}$$

$$\begin{aligned} \gamma_{a\pi\eta} &= \frac{\sqrt{2}}{F_\pi} a_p \left(m_{\rm BARE}^2(a_0) - m_\eta^2 \right), \quad \gamma_{a\pi\eta'} = \frac{\sqrt{2}}{F_\pi} b_p \left(m_{\rm BARE}^2(a_0) - m_{\eta'}^2 \right), \\ \gamma_{\sigma\pi\pi} &= \frac{1}{F_\pi} a_s \left(m_{\rm BARE}^2(\sigma) - m_\pi^2 \right), \quad \gamma_{f_0\pi\pi} = \frac{1}{F_\pi} b_s \left(m_{\rm BARE}^2(f_0) - m_\pi^2 \right). \end{aligned} \tag{A4}$$

For η' decay we will also need:

$$\begin{aligned} \gamma_{\sigma\eta\eta'} = \quad & -\frac{1}{(2F_K - F_\pi)F_\pi^2} a_p b_p \Bigg[-2 m_{\rm BARE}^2(\sigma) a_s^2 b_s F_\pi^2 + \sqrt{2} m_{\rm BARE}^2(\sigma) a_s^3 F_\pi (-2F_K + F_\pi) \\ & + 2 b_s F_\pi \Big(- m_{\rm BARE}^2(\sigma) b_s^2 F_\pi + b_p^2 F_\pi m_\eta^2 + a_p^2 F_\pi m_{\eta'}^2 - \sqrt{2} a_p b_p (2F_K - F_\pi)(m_\eta^2 - m_{\eta'}^2) \Big) \\ & + a_s \Bigg(\sqrt{2} m_{\rm BARE}^2(\sigma) b_s^2 F_\pi (-2F_K + F_\pi) - a_p b_p (4F_K^2 - 4F_K F_\pi + 3F_\pi^2)(m_\eta^2 - m_{\eta'}^2) \\ & + \sqrt{2} a_p^2 (2F_K - F_\pi) F_\pi (2m_\eta^2 - m_{\eta'}^2) + \sqrt{2}(2F_K - F_\pi) F_\pi \Big(- b_p^2 (m_\eta^2 - 2m_{\eta'}^2) + 18(2F_K - F_\pi) V_4 \Big) \Bigg) \Bigg], \end{aligned} \tag{A5}$$

$$\begin{aligned} \gamma_{f_0\eta\eta'} = \quad & -\frac{1}{(2F_K - F_\pi)F_\pi^2} a_p b_p \Big[2 m_{\rm BARE}^2(f_0) a_s^3 F_\pi^2 + \sqrt{2} m_{\rm BARE}^2(f_0) a_s^2 b_s F_\pi (-2F_K + F_\pi) \\ & + 2 a_s F_\pi \Big(m_{\rm BARE}^2(f_0) b_s^2 F_\pi - b_p^2 F_\pi m_\eta^2 - a_p^2 F_\pi m_{\eta'}^2 + \sqrt{2} a_p b_p (2F_K - F_\pi)(m_\eta^2 - m_{\eta'}^2) \Big) \\ & + b_s \Big(\sqrt{2} m_{\rm BARE}^2(f_0) b_s^2 F_\pi (-2F_K + F_\pi) - a_p b_p (4F_K^2 - 4F_K F_\pi + 3F_\pi^2)(m_\eta^2 - m_{\eta'}^2) \\ & + \sqrt{2} a_p^2 (2F_K - F_\pi) F_\pi (2m_\eta^2 - m_{\eta'}^2) + \sqrt{2}(2F_K - F_\pi) F_\pi (-b_p^2 (m_\eta^2 - 2m_{\eta'}^2) \\ & + 18(2F_K - F_\pi) V_4) \Big) \Big]. \end{aligned} \tag{A6}$$

With five inputs of $m_\pi = 137$ MeV, $m_K = 493.677 \pm 0.016$ MeV, $m_\eta = 547.853 \pm 0.024$ MeV, $m_{\eta'} = 957.78 \pm 0.06$ MeV, and $F_\pi = 131$ MeV, we find the five Lagrangian parameters: $\alpha_1 = 0.065$ GeV, $\alpha_3 = 0.13$ GeV, $A_1 = 0.00061$ GeV^3, $A_3 = 0.024$ GeV^3 and $V_4 = -0.23$ (in addition, these inputs result in $\theta_p = 6.64^\circ$, and $F_K/F_\pi = 1.53$). Together with the "bare" scalar masses found from fit to pion-pion $I = J = 0$ scattering amplitude [89]: $m_{\rm BARE}(\sigma) = 0.847\,{\rm GeV}$, $m_{\rm BARE}(f_0) = 1.3\,{\rm GeV}$, $m_{\rm BARE}(a_0) = 1.1\,{\rm GeV}$ and $\theta_s = -6.1^\circ$, we find the numerical values of the coupling constants:

$$\begin{aligned}
\gamma_{\sigma\pi\pi} &= 3.53\,{\rm GeV},\\
\gamma_{f_0\pi\pi} &= 9.57\,{\rm GeV},\\
\gamma_{a_0\pi\eta} &= 4.71\,{\rm GeV},\\
\gamma_{a_0\pi\eta'} &= 2.77\,{\rm GeV},\\
\gamma_{\sigma\eta\eta'} &= -0.56\,{\rm GeV},\\
\gamma_{f_0\eta\eta'} &= 2.94\,{\rm GeV},\\
\gamma^{(4)} &= 78.69\,{\rm GeV}.
\end{aligned} \tag{A7}$$

Appendix B: three- and four-point bare couplings

$$\left\langle \frac{\partial^3 V}{\partial(S_1^2)_1 \partial(\phi_2^1)_1 \partial\eta_a} \right\rangle = \frac{4\sqrt{2}\Big(2c_4^a\alpha_1^5\beta_1 + c_4^a\alpha_1^4\alpha_3\beta_3 + 2c_3\alpha_3\beta_3\gamma_1^2 + 2c_3\alpha_1\beta_1\gamma_1(1+\gamma_1)\Big)}{\alpha_1^3(2\alpha_1\beta_1+\alpha_3\beta_3)}, \tag{B1}$$

$$\left\langle \frac{\partial^3 V}{\partial(S_1^2)_1 \partial(\phi_2^1)_2 \partial\eta_a} \right\rangle = -\frac{8\sqrt{2}c_3\,(-1+\gamma_1)\left(\alpha_3\beta_3\gamma_1 + \alpha_1\beta_1\,(1+\gamma_1)\right)}{\alpha_1\,(2\alpha_1\beta_1+\alpha_3\beta_3)^{\,2}}, \tag{B2}$$

$$\left\langle \frac{\partial^3 V}{\partial(S_1^2)_2 \partial(\phi_2^1)_1 \partial\eta_a} \right\rangle = \frac{8\sqrt{2}c_3\,(-1+\gamma_1)\left(\alpha_3\beta_3\gamma_1 + \alpha_1\beta_1\,(1+\gamma_1)\right)}{\alpha_1\,(2\alpha_1\beta_1+\alpha_3\beta_3)^{\,2}}, \tag{B3}$$

$$\left\langle \frac{\partial^3 V}{\partial(S_1^2)_1 \partial(\phi_2^1)_1 \partial\eta_b} \right\rangle = \frac{8c_3\gamma_1\,(\alpha_3\beta_3 + 2\alpha_1\beta_1\gamma_1)}{\alpha_1^2\alpha_3\,(2\alpha_1\beta_1+\alpha_3\beta_3)}, \tag{B4}$$

$$\left\langle \frac{\partial^3 V}{\partial(S_1^2)_1 \partial(\phi_2^1)_2 \partial\eta_b} \right\rangle = 4e_3^a - \frac{8c_3\,(-1+\gamma_1)\,(\alpha_3\beta_3 + 2\alpha_1\beta_1\gamma_1)}{\alpha_3\,(2\alpha_1\beta_1+\alpha_3\beta_3)^{\,2}}, \tag{B5}$$

$$\left\langle \frac{\partial^3 V}{\partial(S_1^2)_2 \partial(\phi_2^1)_1 \partial\eta_b} \right\rangle = 4e_3^a + \frac{8c_3\,(-1+\gamma_1)\,(\alpha_3\beta_3 + 2\alpha_1\beta_1\gamma_1)}{\alpha_3\,(2\alpha_1\beta_1+\alpha_3\beta_3)^{\,2}}, \tag{B6}$$

$$\left\langle \frac{\partial^3 V}{\partial(S_1^2)_1 \partial(\phi_2^1)_1 \partial\eta_c} \right\rangle = \frac{8\sqrt{2}c_3\,(-1+\gamma_1)\,\gamma_1}{\alpha_1\,(2\alpha_1\beta_1+\alpha_3\beta_3)}, \tag{B7}$$

$$\left\langle \frac{\partial^3 V}{\partial(S_1^2)_1 \partial(\phi_2^1)_2 \partial\eta_c} \right\rangle = -\frac{8\sqrt{2}c_3\alpha_1\,(-1+\gamma_1)^{\,2}}{(2\alpha_1\beta_1+\alpha_3\beta_3)^{\,2}}, \tag{B8}$$

$$\left\langle \frac{\partial^3 V}{\partial(S_1^2)_2 \partial(\phi_2^1)_1 \partial\eta_c} \right\rangle = \frac{8\sqrt{2}c_3\alpha_1\,(-1+\gamma_1)^{\,2}}{(2\alpha_1\beta_1+\alpha_3\beta_3)^{\,2}}, \tag{B9}$$

$$\left\langle \frac{\partial^3 V}{\partial(S_1^2)_1 \partial(\phi_2^1)_1 \partial\eta_d} \right\rangle = \frac{8e_3^a\alpha_1^3\beta_1 + 4e_3^a\alpha_1^2\alpha_3\beta_3 + 8c_3\alpha_3\,(-1+\gamma_1)\,\gamma_1}{\alpha_1^2\,(2\alpha_1\beta_1+\alpha_3\beta_3)}, \tag{B10}$$

$$\left\langle \frac{\partial^3 V}{\partial(S_1^2)_1 \partial(\phi_2^1)_2 \partial\eta_d} \right\rangle = -\frac{8c_3\alpha_3\,(-1+\gamma_1)^{\,2}}{(2\alpha_1\beta_1+\alpha_3\beta_3)^{\,2}}, \tag{B11}$$

$$\left\langle \frac{\partial^3 V}{\partial(S_1^2)_2 \partial(\phi_2^1)_1 \partial\eta_d} \right\rangle = \frac{8c_3\alpha_3\,(-1+\gamma_1)^{\,2}}{(2\alpha_1\beta_1+\alpha_3\beta_3)^{\,2}}, \tag{B12}$$

$$\left\langle \frac{\partial^3 V}{\partial (S_2^3)_1 \partial (\phi_1^2)_1 \partial (\phi_3^1)_1} \right\rangle = 4\alpha_3 c_4^a, \tag{B13}$$

$$\left\langle \frac{\partial^3 V}{\partial (S_2^3)_2 \partial (\phi_1^2)_1 \partial (\phi_3^1)_1} \right\rangle = \left\langle \frac{\partial^3 V}{\partial (S_2^3)_1 \partial (\phi_1^2)_1 \partial (\phi_3^1)_2} \right\rangle = \left\langle \frac{\partial^3 V}{\partial (S_2^3)_1 \partial (\phi_1^2)_2 \partial (\phi_3^1)_1} \right\rangle = -4e_3^a, \tag{B14}$$

$$\begin{aligned} \left\langle \frac{\partial^3 V}{\partial f_a \partial \eta_a \partial \eta_a} \right\rangle = {} & \frac{1}{\alpha_1^3 \left(2\alpha_1\beta_1 + \alpha_3\beta_3\right)^3} 4\sqrt{2}\Big(8c_4^a\alpha_1^7\beta_1^3 + 12c_4^a\alpha_1^6\alpha_3\beta_1^2\beta_3 + 6c_4^a\alpha_1^5\alpha_3^2\beta_1\beta_3^2 \\ & + c_4^a\alpha_1^4\alpha_3^3\beta_3^3 + 4c_3\alpha_3^3\beta_3^3\gamma_1^2 + 24c_3\alpha_1^2\alpha_3\beta_1^2\beta_3\gamma_1\left(1+\gamma_1\right) \\ & + 8c_3\alpha_1^3\beta_1^3\left(1+\gamma_1\right)^2 + 4c_3\alpha_1\alpha_3^2\beta_1\beta_3^2\gamma_1\left(1+5\gamma_1\right)\Big), \end{aligned} \tag{B15}$$

$$\left\langle \frac{\partial^3 V}{\partial f_a \partial \eta_a \partial \eta_b} \right\rangle = \frac{8c_3\Big(6\alpha_1\alpha_3^2\beta_1\beta_3^2\gamma_1 + \alpha_3^3\beta_3^3\gamma_1 + 4\alpha_1^3\beta_1^3\gamma_1\left(1+\gamma_1\right) + 2\alpha_1^2\alpha_3\beta_1^2\beta_3\left(2+\gamma_1+3\gamma_1^2\right)\Big)}{\alpha_1^2\alpha_3\left(2\alpha_1\beta_1+\alpha_3\beta_3\right)^3}, \tag{B16}$$

$$\left\langle \frac{\partial^3 V}{\partial f_a \partial \eta_a \partial \eta_c} \right\rangle = \frac{8\sqrt{2}c_3\beta_1\left(-1+\gamma_1\right)\Big(2\alpha_1\beta_1\left(1+\gamma_1\right) + \alpha_3\beta_3\left(-1+3\gamma_1\right)\Big)}{\left(2\alpha_1\beta_1+\alpha_3\beta_3\right)^3}, \tag{B17}$$

$$\begin{aligned} \left\langle \frac{\partial^3 V}{\partial f_a \partial \eta_a \partial \eta_d} \right\rangle = {} & \frac{-4}{\alpha_1^2\left(2\alpha_1\beta_1+\alpha_3\beta_3\right)^3}\Big[8e_3^a\alpha_1^5\beta_1^3 + 12e_3^a\alpha_1^4\alpha_3\beta_1^2\beta_3 + 6e_3^a\alpha_1^3\alpha_3^2\beta_1\beta_3^2 \\ & - 12c_3\alpha_1\alpha_3^2\beta_1\beta_3\left(-1+\gamma_1\right)\gamma_1 - 2c_3\alpha_3^3\beta_3^2\left(-1+\gamma_1\right)\gamma_1 \\ & + \alpha_1^2\alpha_3\Big(e_3^a\alpha_3^2\beta_3^3 - 8c_3\beta_1^2(-1+\gamma_1^2)\Big)\Big], \end{aligned} \tag{B18}$$

$$\left\langle \frac{\partial^3 V}{\partial f_a \partial \eta_b \partial \eta_b} \right\rangle = -\frac{16\sqrt{2}c_3\beta_1\beta_3\left(-1+\gamma_1\right)\left(\alpha_3\beta_3+2\alpha_1\beta_1\gamma_1\right)}{\alpha_3\left(2\alpha_1\beta_1+\alpha_3\beta_3\right)^3}, \tag{B19}$$

$$\begin{aligned} \left\langle \frac{\partial^3 V}{\partial f_a \partial \eta_b \partial \eta_c} \right\rangle = {} & \frac{-4}{\left(2\alpha_1\beta_1+\alpha_3\beta_3\right)^3}\Big[8e_3^a\alpha_1^3\beta_1^3 + 12e_3^a\alpha_1^2\alpha_3\beta_1^2\beta_3 + \alpha_3\beta_3^2\Big(e_3^a\alpha_3^2\beta_3 + 2c_3\left(-1+\gamma_1\right)\Big) \\ & + 2\alpha_1\beta_1\beta_3\Big(3e_3^a\alpha_3^2\beta_3 + 2c_3(1-3\gamma_1+2\gamma_1^2)\Big)\Big], \end{aligned} \tag{B20}$$

$$\left\langle \frac{\partial^3 V}{\partial f_a \partial \eta_b \partial \eta_d} \right\rangle = \frac{8\sqrt{2}c_3\beta_1\left(-1+\gamma_1\right)\Big(-\alpha_3\beta_3\left(-2+\gamma_1\right) + 2\alpha_1\beta_1\gamma_1\Big)}{\left(2\alpha_1\beta_1+\alpha_3\beta_3\right)^3}, \tag{B21}$$

$$\left\langle \frac{\partial^3 V}{\partial f_a \partial \eta_c \partial \eta_c} \right\rangle = -\frac{16\sqrt{2}c_3\alpha_1\alpha_3\beta_3\left(-1+\gamma_1\right)^2}{\left(2\alpha_1\beta_1+\alpha_3\beta_3\right)^3}, \tag{B22}$$

$$\left\langle \frac{\partial^3 V}{\partial f_a \partial \eta_c \partial \eta_d} \right\rangle = -\frac{8c_3\alpha_3\left(-2\alpha_1\beta_1+\alpha_3\beta_3\right)\left(-1+\gamma_1\right)^2}{\left(2\alpha_1\beta_1+\alpha_3\beta_3\right)^3}, \tag{B23}$$

$$\left\langle \frac{\partial^3 V}{\partial f_a \partial \eta_d \partial \eta_d} \right\rangle = \frac{16\sqrt{2}c_3\alpha_3^2\beta_1\left(-1+\gamma_1\right)^2}{\left(2\alpha_1\beta_1+\alpha_3\beta_3\right)^3}, \tag{B24}$$

$$\left\langle \frac{\partial^3 V}{\partial f_b \partial \eta_a \partial \eta_a} \right\rangle = -\frac{32c_3\beta_1\beta_3\left(-1+\gamma_1\right)\Big(\alpha_3\beta_3\gamma_1 + \alpha_1\beta_1\left(1+\gamma_1\right)\Big)}{\alpha_1\left(2\alpha_1\beta_1+\alpha_3\beta_3\right)^3}, \tag{B25}$$

$$\begin{aligned} \left\langle \frac{\partial^3 V}{\partial f_b \partial \eta_a \partial \eta_b} \right\rangle = {} & \frac{1}{\alpha_1\alpha_3^2\left(2\alpha_1\beta_1+\alpha_3\beta_3\right)^3}\Big[8\sqrt{2}c_3\Big(\alpha_3^3\beta_3^3\gamma_1 + 4\alpha_1^3\beta_1^3\gamma_1\left(1+\gamma_1\right) \\ & + 6\alpha_1^2\alpha_3\beta_1^2\beta_3\gamma_1\left(1+\gamma_1\right) + 2\alpha_1\alpha_3^2\beta_1\beta_3^2(1+2\gamma_1^2)\Big)\Big], \end{aligned} \tag{B26}$$

$$\left\langle \frac{\partial^3 V}{\partial f_b \partial \eta_a \partial \eta_c} \right\rangle = \frac{-4}{\left(2\alpha_1\beta_1+\alpha_3\beta_3\right)^3}\Big[8e_3^a\alpha_1^3\beta_1^3 + 12e_3^a\alpha_1^2\alpha_3\beta_1^2\beta_3 + 2\alpha_1\beta_1\beta_3\Big(3e_3^a\alpha_3^2\beta_3 - 4c_3\left(-1+\gamma_1\right)\Big)$$

$$+\alpha_3\beta_3^2\Big(e_3^a\alpha_3^2\beta_3-4c_3\left(-1+\gamma_1\right)\gamma_1\Big)\Big], \tag{B27}$$

$$\left\langle\frac{\partial^3 V}{\partial f_b\partial\eta_a\partial\eta_d}\right\rangle = -\frac{8\sqrt{2}c_3\beta_1\left(-1+\gamma_1\right)\Big(2\alpha_1\beta_1\left(1+\gamma_1\right)+\alpha_3\beta_3\left(-1+3\gamma_1\right)\Big)}{\left(2\alpha_1\beta_1+\alpha_3\beta_3\right)^3}, \tag{B28}$$

$$\left\langle\frac{\partial^3 V}{\partial f_b\partial\eta_b\partial\eta_b}\right\rangle = \frac{8}{\alpha_3^3\left(2\alpha_1\beta_1+\alpha_3\beta_3\right)^3}\Big[\alpha_3^3\left(2c_3+c_4^a\alpha_3^4\right)\beta_3^3+6\alpha_1\alpha_3^2\beta_1\beta_3^2\left(c_4^a\alpha_3^4+2c_3\gamma_1\right)$$
$$+8\alpha_1^3\beta_1^3\left(c_4^a\alpha_3^4+2c_3\gamma_1^2\right)+4\alpha_1^2\alpha_3\beta_1^2\beta_3\Big(3c_4^a\alpha_3^4+\,2c_3\gamma_1(1+2\gamma_1)\Big)\Big], \tag{B29}$$

$$\left\langle\frac{\partial^3 V}{\partial f_b\partial\eta_b\partial\eta_c}\right\rangle = \frac{16\sqrt{2}c_3\alpha_1\left(-1+\gamma_1\right)\left(\alpha_3^2\beta_3^2+2\alpha_1^2\beta_1^2\gamma_1+3\alpha_1\alpha_3\beta_1\beta_3\gamma_1\right)}{\alpha_3^2\left(2\alpha_1\beta_1+\alpha_3\beta_3\right)^3}, \tag{B30}$$

$$\left\langle\frac{\partial^3 V}{\partial f_b\partial\eta_b\partial\eta_d}\right\rangle = \frac{8c_3\beta_3\left(-1+\gamma_1\right)\Big(\alpha_3\beta_3+2\alpha_1\beta_1\left(-1+2\gamma_1\right)\Big)}{\left(2\alpha_1\beta_1+\alpha_3\beta_3\right)^3}, \tag{B31}$$

$$\left\langle\frac{\partial^3 V}{\partial f_b\partial\eta_c\partial\eta_c}\right\rangle = \frac{32c_3\alpha_1^2\beta_3\left(-1+\gamma_1\right)^2}{\left(2\alpha_1\beta_1+\alpha_3\beta_3\right)^3}, \tag{B32}$$

$$\left\langle\frac{\partial^3 V}{\partial f_b\partial\eta_c\partial\eta_d}\right\rangle = -\frac{8\sqrt{2}c_3\alpha_1\left(2\alpha_1\beta_1-\alpha_3\beta_3\right)\left(-1+\gamma_1\right)^2}{\left(2\alpha_1\beta_1+\alpha_3\beta_3\right)^3}, \tag{B33}$$

$$\left\langle\frac{\partial^3 V}{\partial f_b\partial\eta_d\partial\eta_d}\right\rangle = -\frac{32c_3\alpha_1\alpha_3\beta_1\left(-1+\gamma_1\right)^2}{\left(2\alpha_1\beta_1+\alpha_3\beta_3\right)^3}, \tag{B34}$$

$$\left\langle\frac{\partial^3 V}{\partial f_c\partial\eta_a\partial\eta_a}\right\rangle = \frac{16\sqrt{2}c_3\alpha_3\beta_3\left(-1+\gamma_1\right)\Big(\alpha_3\beta_3\gamma_1+\alpha_1\beta_1\left(1+\gamma_1\right)\Big)}{\alpha_1\left(2\alpha_1\beta_1+\alpha_3\beta_3\right)^3}, \tag{B35}$$

$$\left\langle\frac{\partial^3 V}{\partial f_c\partial\eta_a\partial\eta_b}\right\rangle = -\frac{4\Big(8e_3^a\alpha_1^3\beta c_3\left(-1+\gamma_1\right)\Big)+\alpha_3\beta_3^2\Big(e_3^a\alpha_3^2\beta_3+2c_3(1-3\gamma_1+2\gamma_1^2)\Big)}{\left(2\alpha_1\beta_1+\alpha_3\beta_3\right)^3}, \tag{B36}$$

$$\left\langle\frac{\partial^3 V}{\partial f_c\partial\eta_a\partial\eta_c}\right\rangle = \frac{8\sqrt{2}c_3\alpha_1\left(-1+\gamma_1\right)\Big(2\alpha_1\beta_1(1+\gamma_1)+\alpha_3\beta_3\left(-1+3\gamma_1\right)\Big)}{\left(2\alpha_1\beta_1+\alpha_3\beta_3\right)^3}, \tag{B37}$$

$$\left\langle\frac{\partial^3 V}{\partial f_c\partial\eta_a\partial\eta_d}\right\rangle = \frac{8c_3\alpha_3\left(-1+\gamma_1\right)\Big(2\alpha_1\beta_1\left(1+\gamma_1\right)+\alpha_3\beta_3\left(-1+3\gamma_1\right)\Big)}{\left(2\alpha_1\beta_1+\alpha_3\beta_3\right)^3}, \tag{B38}$$

$$\left\langle\frac{\partial^3 V}{\partial f_c\partial\eta_b\partial\eta_b}\right\rangle = -\frac{16\sqrt{2}c_3\alpha_1\beta_3\left(-1+\gamma_1\right)\left(\alpha_3\beta_3+2\alpha_1\beta_1\gamma_1\right)}{\alpha_3\left(2\alpha_1\beta_1+\alpha_3\beta_3\right)^3}, \tag{B39}$$

$$\left\langle\frac{\partial^3 V}{\partial f_c\partial\eta_b\partial\eta_c}\right\rangle = \frac{16c_3\alpha_1^2\left(-1+\gamma_1\right)\Big(-\alpha_3\beta_3\left(-2+\gamma_1\right)+2\alpha_1\beta_1\gamma_1\Big)}{\alpha_3\left(2\alpha_1\beta_1+\alpha_3\beta_3\right)^3}, \tag{B40}$$

$$\left\langle\frac{\partial^3 V}{\partial f_c\partial\eta_b\partial\eta_d}\right\rangle = \frac{8\sqrt{2}c_3\alpha_1\left(-1+\gamma_1\right)\Big(-\alpha_3\beta_3\left(-2+\gamma_1\right)+2\alpha_1\beta_1\gamma_1\Big)}{\left(2\alpha_1\beta_1+\alpha_3\beta_3\right)^3}, \tag{B41}$$

$$\left\langle\frac{\partial^3 V}{\partial f_c\partial\eta_c\partial\eta_c}\right\rangle = \frac{32\sqrt{2}c_3\alpha_1^3\left(-1+\gamma_1\right)^2}{\left(2\alpha_1\beta_1+\alpha_3\beta_3\right)^3}, \tag{B42}$$

$$\left\langle\frac{\partial^3 V}{\partial f_c\partial\eta_c\partial\eta_d}\right\rangle = \frac{32c_3\alpha_1^2\alpha_3\left(-1+\gamma_1\right)^2}{\left(2\alpha_1\beta_1+\alpha_3\beta_3\right)^3}, \tag{B43}$$

$$\left\langle \frac{\partial^3 V}{\partial f_c \partial \eta_d \partial \eta_d} \right\rangle = \frac{16\sqrt{2} c_3 \alpha_1 \alpha_3^2 \left(-1+\gamma_1\right)^2}{\left(2\alpha_1\beta_1+\alpha_3\beta_3\right)^3}, \tag{B44}$$

$$\left\langle \frac{\partial^3 V}{\partial f_d \partial \eta_a \partial \eta_a} \right\rangle = \frac{-4}{\alpha_1 \left(2\alpha_1\beta_1+\alpha_3\beta_3\right)^3}\Bigg[\Bigg(8e_3^a\alpha_1^4\beta_1^3+12e_3^a\alpha_1^3\alpha_3\beta_1^2\beta_3+6e_3^a\alpha_1^2\alpha_3^2\beta_1\beta_3^2 +8c_3\alpha_3^2\beta_1\beta_3\left(-1+\gamma_1\right)\gamma_1+\alpha_1\alpha_3\Big(e_3^a\alpha_3^2\beta_3^3+8c_3\beta_1^2(-1+\gamma_1^2)\Big)\Bigg)\Bigg], \tag{B45}$$

$$\left\langle \frac{\partial^3 V}{\partial f_d \partial \eta_a \partial \eta_b} \right\rangle = \frac{8\sqrt{2} c_3 \beta_1 \left(-1+\gamma_1\right)\Big(2\alpha_1\beta_1+\alpha_3\beta_3\left(-1+2\gamma_1\right)\Big)}{\left(2\alpha_1\beta_1+\alpha_3\beta_3\right)^3}, \tag{B46}$$

$$\left\langle \frac{\partial^3 V}{\partial f_d \partial \eta_a \partial \eta_c} \right\rangle = \frac{16 c_3 \alpha_3 \left(-1+\gamma_1\right)\left(2\alpha_1\beta_1+\alpha_3\beta_3\gamma_1\right)}{\left(2\alpha_1\beta_1+\alpha_3\beta_3\right)^3}, \tag{B47}$$

$$\left\langle \frac{\partial^3 V}{\partial f_d \partial \eta_a \partial \eta_d} \right\rangle = \frac{8\sqrt{2} c_3 \alpha_3^2 \left(-1+\gamma_1\right)\left(2\alpha_1\beta_1+\alpha_3\beta_3\gamma_1\right)}{\alpha_1\left(2\alpha_1\beta_1+\alpha_3\beta_3\right)^3}, \tag{B48}$$

$$\left\langle \frac{\partial^3 V}{\partial f_d \partial \eta_b \partial \eta_b} \right\rangle = \frac{32 c_3 \alpha_1 \beta_1 \left(-1+\gamma_1\right)\left(\alpha_3\beta_3+2\alpha_1\beta_1\gamma_1\right)}{\alpha_3\left(2\alpha_1\beta_1+\alpha_3\beta_3\right)^3}, \tag{B49}$$

$$\left\langle \frac{\partial^3 V}{\partial f_d \partial \eta_b \partial \eta_c} \right\rangle = \frac{8\sqrt{2} c_3 \alpha_1 \left(-1+\gamma_1\right)\Big(\alpha_3\beta_3+2\alpha_1\beta_1\left(-1+2\gamma_1\right)\Big)}{\left(2\alpha_1\beta_1+\alpha_3\beta_3\right)^3}, \tag{B50}$$

$$\left\langle \frac{\partial^3 V}{\partial f_d \partial \eta_b \partial \eta_d} \right\rangle = \frac{8 c_3 \alpha_3 \left(-1+\gamma_1\right)\Big(\alpha_3\beta_3+2\alpha_1\beta_1\left(-1+2\gamma_1\right)\Big)}{\left(2\alpha_1\beta_1+\alpha_3\beta_3\right)^3}, \tag{B51}$$

$$\left\langle \frac{\partial^3 V}{\partial f_d \partial \eta_c \partial \eta_c} \right\rangle = \frac{32 c_3 \alpha_1^2 \alpha_3 \left(-1+\gamma_1\right)^2}{\left(2\alpha_1\beta_1+\alpha_3\beta_3\right)^3}, \tag{B52}$$

$$\left\langle \frac{\partial^3 V}{\partial f_d \partial \eta_c \partial \eta_d} \right\rangle = \frac{16\sqrt{2} c_3 \alpha_1 \alpha_3^2 \left(-1+\gamma_1\right)^2}{\left(2\alpha_1\beta_1+\alpha_3\beta_3\right)^3}, \tag{B53}$$

$$\left\langle \frac{\partial^3 V}{\partial f_d \partial \eta_d \partial \eta_d} \right\rangle = \frac{16 c_3 \alpha_3^3 \left(-1+\gamma_1\right)^2}{\left(2\alpha_1\beta_1+\alpha_3\beta_3\right)^3}, \tag{B54}$$

$$\left\langle \frac{\partial^4 V}{\partial \eta_a \partial \eta_a \partial (\phi_1^2)_1 \partial (\phi_2^1)_1} \right\rangle = \frac{4\Big(6c_4^a\alpha_1^5\beta_1+3c_4^a\alpha_1^4\alpha_3\beta_3+8c_3\alpha_3\beta_3\gamma_1^2+8c_3\alpha_1\beta_1\gamma_1\left(1+\gamma_1\right)\Big)}{\alpha_1^4\left(2\alpha_1\beta_1+\alpha_3\beta_3\right)}, \tag{B55}$$

$$\left\langle \frac{\partial^4 V}{\partial \eta_a \partial \eta_a \partial (\phi_1^2)_1 \partial (\phi_2^1)_2} \right\rangle = \left\langle \frac{\partial^4 V}{\partial \eta_a \partial \eta_a \partial (\phi_1^2)_2 \partial (\phi_2^1)_1} \right\rangle = -\frac{32 c_3 \beta_1 \left(-1+\gamma_1\right)\Big(\alpha_3\beta_3\gamma_1+\alpha_1\beta_1\left(1+\gamma_1\right)\Big)}{\alpha_1\left(2\alpha_1\beta_1+\alpha_3\beta_3\right)^3}, \tag{B56}$$

$$\left\langle \frac{\partial^4 V}{\partial \eta_a \partial \eta_b \partial (\phi_1^2)_1 \partial (\phi_2^1)_1} \right\rangle = \frac{8\sqrt{2} c_3 \gamma_1 \left(\alpha_3\beta_3+2\alpha_1\beta_1\gamma_1\right)}{\alpha_1^3\alpha_3\left(2\alpha_1\beta_1+\alpha_3\beta_3\right)}, \tag{B57}$$

$$\left\langle \frac{\partial^4 V}{\partial \eta_a \partial \eta_b \partial (\phi_1^2)_1 \partial (\phi_2^1)_2} \right\rangle = \left\langle \frac{\partial^4 V}{\partial \eta_a \partial \eta_b \partial (\phi_1^2)_2 \partial (\phi_2^1)_1} \right\rangle = \frac{-8\sqrt{2} c_3 \left(-1+\gamma_1\right)\Big(2\alpha_1^2\beta_1^2\gamma_1+\alpha_3^2\beta_3^2\gamma_1+\alpha_1\alpha_3\beta_1\beta_3\left(2+\gamma_1\right)\Big)}{\alpha_1\alpha_3\left(2\alpha_1\beta_1+\alpha_3\beta_3\right)^3}, \tag{B58}$$

$$\left\langle \frac{\partial^4 V}{\partial \eta_a \partial \eta_c \partial (\phi_1^2)_1 \partial (\phi_2^1)_1} \right\rangle = \frac{16 c_3 \left(-1+\gamma_1\right)\gamma_1}{\alpha_1^2\left(2\alpha_1\beta_1+\alpha_3\beta_3\right)}, \tag{B59}$$

$$\left\langle \frac{\partial^4 V}{\partial \eta_a \partial \eta_c \partial (\phi_1^2)_1 \partial (\phi_2^1)_2} \right\rangle = \left\langle \frac{\partial^4 V}{\partial \eta_a \partial \eta_c \partial (\phi_1^2)_2 \partial (\phi_2^1)_1} \right\rangle = \frac{16 c_3 \left(-1+\gamma_1\right)\left(2\alpha_1\beta_1+\alpha_3\beta_3\gamma_1\right)}{\left(2\alpha_1\beta_1+\alpha_3\beta_3\right)^3}, \tag{B60}$$

$$\left\langle \frac{\partial^4 V}{\partial\eta_a\partial\eta_d\partial(\phi_1^2)_1\partial(\phi_2^1)_1}\right\rangle = \frac{8\sqrt{2}c_3\alpha_3\left(-1+\gamma_1\right)\gamma_1}{\alpha_1^3\left(2\alpha_1\beta_1+\alpha_3\beta_3\right)}, \tag{B61}$$

$$\left\langle \frac{\partial^4 V}{\partial\eta_a\partial\eta_d\partial(\phi_1^2)_1\partial(\phi_2^1)_2}\right\rangle = \left\langle \frac{\partial^4 V}{\partial\eta_a\partial\eta_d\partial(\phi_1^2)_2\partial(\phi_2^1)_1}\right\rangle = \frac{8\sqrt{2}c_3\alpha_3\left(-1+\gamma_1\right)\left(2\alpha_1\beta_1+\alpha_3\beta_3\gamma_1\right)}{\alpha_1\left(2\alpha_1\beta_1+\alpha_3\beta_3\right)^3}, \tag{B62}$$

$$\left\langle \frac{\partial^4 V}{\partial\eta_b\partial\eta_b\partial(\phi_1^2)_1\partial(\phi_2^1)_2}\right\rangle = \left\langle \frac{\partial^4 V}{\partial\eta_b\partial\eta_b\partial(\phi_1^2)_2\partial(\phi_2^1)_1}\right\rangle = -\frac{16c_3\beta_3\left(-1+\gamma_1\right)\left(\alpha_3\beta_3+2\alpha_1\beta_1\gamma_1\right)}{\alpha_3\left(2\alpha_1\beta_1+\alpha_3\beta_3\right)^3}, \tag{B63}$$

$$\left\langle \frac{\partial^4 V}{\partial\eta_b\partial\eta_c\partial(\phi_1^2)_1\partial(\phi_2^1)_2}\right\rangle = \left\langle \frac{\partial^4 V}{\partial\eta_b\partial\eta_b\partial(\phi_1^2)_2\partial(\phi_2^1)_1}\right\rangle = \frac{8\sqrt{2}c_3\alpha_1\left(-1+\gamma_1\right)\Big(-\alpha_3\beta_3\left(-2+\gamma_1\right)+2\alpha_1\beta_1\gamma_1\Big)}{\alpha_3\left(2\alpha_1\beta_1+\alpha_3\beta_3\right)^3}, \tag{B64}$$

$$\left\langle \frac{\partial^4 V}{\partial\eta_b\partial\eta_d\partial(\phi_1^2)_1\partial(\phi_2^1)_2}\right\rangle = \left\langle \frac{\partial^4 V}{\partial\eta_b\partial\eta_d\partial(\phi_1^2)_2\partial(\phi_2^1)_1}\right\rangle = \frac{8c_3\left(-1+\gamma_1\right)\Big(-\alpha_3\beta_3\left(-2+\gamma_1\right)+2\alpha_1\beta_1\gamma_1\Big)}{\left(2\alpha_1\beta_1+\alpha_3\beta_3\right)^3}, \tag{B65}$$

$$\left\langle \frac{\partial^4 V}{\partial\eta_c\partial\eta_c\partial(\phi_1^2)_1\partial(\phi_2^1)_2}\right\rangle = \left\langle \frac{\partial^4 V}{\partial\eta_c\partial\eta_c\partial(\phi_1^2)_2\partial(\phi_2^1)_1}\right\rangle = \frac{32c_3\alpha_1^2\left(-1+\gamma_1\right)^2}{\left(2\alpha_1\beta_1+\alpha_3\beta_3\right)^3}, \tag{B66}$$

$$\left\langle \frac{\partial^4 V}{\partial\eta_c\partial\eta_d\partial(\phi_1^2)_1\partial(\phi_2^1)_2}\right\rangle = \left\langle \frac{\partial^4 V}{\partial\eta_c\partial\eta_d\partial(\phi_1^2)_2\partial(\phi_2^1)_1}\right\rangle = \frac{16\sqrt{2}c_3\alpha_1\alpha_3\left(-1+\gamma_1\right)^2}{\left(2\alpha_1\beta_1+\alpha_3\beta_3\right)^3}, \tag{B67}$$

$$\left\langle \frac{\partial^4 V}{\partial\eta_d\partial\eta_d\partial(\phi_1^2)_1\partial(\phi_2^1)_2}\right\rangle = \left\langle \frac{\partial^4 V}{\partial\eta_d\partial\eta_d\partial(\phi_1^2)_2\partial(\phi_2^1)_1}\right\rangle = \frac{16c_3\alpha_3^2\left(-1+\gamma_1\right)^2}{\left(2\alpha_1\beta_1+\alpha_3\beta_3\right)^3}. \tag{B68}$$

Appendix C: Recovering current algebra

In this Appendix we show how the known current algebra result for this decay is obtained from the present model. The four-quark fields are decoupled in the limit $d_2, e_3^a \to 0$ and $\gamma_1 \to 1$, in which:

$$\begin{aligned} m_\pi^2 &= -2c_2 + 4c_4^a\alpha_1^2, \\ m_{f_1}^2 &= m_a^2 = -2c_2 + 12c_4^a\alpha_1^2, \\ m_{f_2}^2 &= -2c_2 + 12c_4^a\alpha_3^2, \\ F_\pi &= 2\alpha_1, \\ m_\eta^2 + m_{\eta'}^2 &= -4c_2 - \frac{16c_3}{\alpha_1^2} + 4c_4^a\alpha_1^2 - \frac{8c_3}{\alpha_3^2} + 4c_4^a\alpha_3^2. \end{aligned} \tag{C1}$$

From the above equations we can solve for the five model parameters:

$$\begin{aligned} \alpha_1 &= \frac{F_\pi}{2}, \\ \alpha_3 &= F_\pi\sqrt{\frac{2m_{f_2}^2 + m_{f_1}^2 - 3m_\pi^2}{12(m_{f_1}^2 - m_\pi^2)}}, \\ c_2 &= \frac{1}{4}(m_{f_1}^2 - 3m_\pi^2), \\ c_3 &= -\frac{F_\pi^2(m_{f_1}^2 + 2m_{f_2}^2 - 3m_\pi^2)\Big(m_{f_1}^2 - m_{f_2}^2 + 3(m_\eta^2 + m_{\eta'}^2 - 2m_\pi^2)\Big)}{96(5m_{f_1}^2 + 4m_{f_1}^2 - 9m_\pi^2)}, \\ c_4^a &= \frac{m_{f_1}^2 - m_\pi^2}{2F_\pi^2}. \end{aligned} \tag{C2}$$

We expect to recover the current algebra result when the scalars are decoupled as a result of becoming very heavy,

i.e. in the limit $m_{f_1} = m_{f_2} = m_f \to \infty$. In this limit,

$$\begin{aligned}
\lim_{m_f\to\infty} \alpha_3 &= \frac{F_\pi}{2}, \\
\lim_{m_f\to\infty} c_2 &= \frac{m_f^2}{4}, \\
\lim_{m_f\to\infty} c_3 &= \frac{-1}{96} F_\pi^2 (m_\eta^2 + m_{\eta'}^2 - 2m_\pi^2) \\
\lim_{m_f\to\infty} c_4^a &= \frac{m_f^2}{2F_\pi^2}
\end{aligned} \tag{C3}$$

The physical vertices (in the limit of $d_2, e_3^a \to 0$ and $\gamma_1 \to 1$) become:

$$\begin{aligned}
\gamma^{(4)} &= 6\, c_4^a \sin(2\theta_p) + \frac{16\, c_3 \sin(2\theta_p)}{\alpha_1^4} + \frac{8\sqrt{2} c_3 \cos(2\theta_p)}{\alpha_1^3 \alpha_3}, \\
\gamma_{f_1\pi\pi} &= 4 c_4^a \alpha_1, \\
\gamma_{f_2\pi\pi} &= 0, \\
\gamma_{f_1\eta\eta'} &= 2\sqrt{2}\, c_4^a \sin(2\theta_p)\alpha_1 + \frac{8\sqrt{2}\, c_3 \sin(2\theta_p)}{\alpha_1^3} + \frac{8\, c_3 \cos(2\theta_p)}{\alpha_1^2 \alpha_3}, \\
\gamma_{f_2\eta\eta'} &= \frac{8\sqrt{2}\, c_3 \cos(2\theta_p)\alpha_3 - 4 \sin(2\theta_p)\alpha_1 (2\, c_3 + c_4^a \alpha_3^4)}{\alpha_1 \alpha_3^3}, \\
\gamma_{a_0\pi\eta} &= \frac{8\sqrt{2}\, c_3 \cos(\theta_p)}{\alpha_1^3} + 4\sqrt{2}\, c_4^a \cos(\theta_p)\alpha_1 - \frac{8\, c_3 \sin(\theta_p)}{\alpha_1^2 \alpha_3}, \\
\gamma_{a_0\pi\eta'} &= \frac{8\sqrt{2}\, c_3 \sin(\theta_p)}{\alpha_1^3} + 4\sqrt{2}\, c_4^a \sin(\theta_p)\alpha_1 + \frac{8\, c_3 \cos(\theta_p)}{\alpha_1^2 \alpha_3},
\end{aligned} \tag{C4}$$

which together with (C3),

$$\begin{aligned}
\gamma^{(4)} &= \frac{1}{3F_\pi^2}\Big[\left(m_\eta^2 + m_{\eta'}^2 - 2m_\pi^2\right)\Big(-4\sqrt{2}\cos(2\theta_p) - 8\sin(2\theta_p)\Big) + 9\left(m_f^2 - m_\pi^2\right)\sin(2\theta_p)\Big] \\
\gamma_{f_1\pi\pi} &= \frac{m_f^2 - m_\pi^2}{F_\pi}, \\
\gamma_{f_1\eta\eta'} &= \frac{1}{3F_\pi}\Big[\left(m_\eta^2 + m_{\eta'}^2 - 2m_\pi^2\right)\Big(-2\cos(2\theta_p) - 2\sqrt{2}\sin(2\theta_p)\Big) + \frac{3}{\sqrt{2}}\left(m_f^2 - m_\pi^2\right)\sin(2\theta_p)\Big], \\
\gamma_{f_2\eta\eta'} &= \frac{2}{3F_\pi}\Big[\left(m_\eta^2 + m_{\eta'}^2 - 2m_\pi^2\right)\Big(-\sqrt{2}\cos(2\theta_p) + \sin(2\theta_p)\Big) - \frac{3}{2}\left(m_f^2 - m_\pi^2\right)\sin(2\theta_p)\Big], \\
\gamma_{a_0\pi\eta} &= \frac{1}{3F_\pi}\Big[\left(m_\eta^2 + m_{\eta'}^2 - 2m_\pi^2\right)\Big(-2\sqrt{2}\cos(\theta_p) + 2\sin(\theta_p)\Big) + 3\sqrt{2}\left(m_f^2 - m_\pi^2\right)\cos(\theta_p)\Big], \\
\gamma_{a_0\pi\eta'} &= \frac{1}{3F_\pi}\Big[\left(m_\eta^2 + m_{\eta'}^2 - 2m_\pi^2\right)\Big(-2\cos(\theta_p) - 2\sqrt{2}\sin(\theta_p)\Big) + 3\sqrt{2}\left(m_f^2 - m_\pi^2\right)\sin(\theta_p)\Big].
\end{aligned} \tag{C5}$$

Each individual decay amplitude inherits the scalar mass dependency via the physical vertices and propagators. The four-point amplitude will have the scalar mass dependency

$$M_{4p} = \xi_0 + \xi_1 m_f^2. \tag{C6}$$

The isosinglet scalar contribution has the general structure

$$M_{f_i} = \sqrt{2}\gamma_{f_i\pi\pi}\gamma_{f_i\eta\eta'} \times (\text{propagator}), \tag{C7}$$

with

$$\begin{aligned}\sqrt{2}\gamma_{f_i\pi\pi}\gamma_{f_i\eta\eta'} &= \rho_0+\rho_1 m_f^2+\rho_2 m_f^4,\\ \text{propagator} &= \frac{1}{m_f^2+x}\simeq\frac{1}{m_f^2}-\frac{x}{m_f^4}+\mathcal{O}(\frac{1}{m_f^6}).\end{aligned}\tag{C8}$$

Thus

$$\lim_{m_f\to\infty} M_{f_i}=\rho_1-x\rho_2+\rho_2 m_f^2.\tag{C9}$$

Similarly for the a_0 contribution

$$M_{a_0}=\gamma_{a_0\pi\eta}\gamma_{a_0\pi\eta'}\big[\frac{1}{m_f^2+y_1}+\frac{1}{m_f^2+y_2}\big],\tag{C10}$$

with

$$\begin{aligned}\gamma_{a_0\pi\eta}\gamma_{a_0\pi\eta'}&=\delta_0+\delta_1 m_f^2+\delta_2 m_f^4,\\ \frac{1}{m_f^2+y_i}&\simeq\frac{1}{m_f^2}-\frac{y_i}{m_f^4}+\mathcal{O}(\frac{1}{m_f^6}).\end{aligned}\tag{C11}$$

Thus

$$\lim_{m_f\to\infty} M_{a_0}=2\,\delta_1-\sum_i y_i\delta_2+2\,\delta_2 m_f^2.\tag{C12}$$

Now putting everything together, we expect:

$$\lim_{m_f\to\infty} M_{\text{total}}=M_{\text{C.A.}}\tag{C13}$$

which implies that the following two sum rules must be upheld

$$\begin{aligned}\xi_0+\rho_1-x\rho_2+2\,\delta_1-\sum_i y_i\delta_2 &= M_{\text{C.A.}},\\ \xi_1+\rho_2+2\,\delta_2 &= 0.\end{aligned}\tag{C14}$$

We find that the second sum-rule is identically upheld, and the first one gives:

$$M_{\text{C.A.}}=\frac{-1}{3F_\pi^2}\left(\sin(2\theta_p)\left(m_\eta^2+m_{\eta'}^2-5m_\pi^2\right)+2\sqrt{2}\cos(2\theta_p)\left(m_\eta^2+m_{\eta'}^2-2m_\pi^2\right)\right).\tag{C15}$$

Since in the decoupling limit $c_3=0$ and $m_f\to\infty$ we have

$$2m_\pi^2\to m_\eta^2+m_{\eta'}^2,\tag{C16}$$

which results in

$$M_{\text{C.A.}}=\frac{m_\pi^2}{F_\pi^2}\sin(2\theta p),\tag{C17}$$

in agreement with Eq. (2.4) of ref. [91].

Acknowledgments

A.H.F. wishes to thank the Physics Dept. of Shiraz University for its hospitality in Summer of 2012 where this work was initiated. A.H.F. also wishes to thank Prof. M. Amaryan for many helpful discussions. The work of J.S. is supported in part by the US DOE under the Contract No. DE-FG-02-85ER 40231.

[1] J. Beringer et al. (Particle Data Group), Phys. Rev. D **86**, 010001 (2012).
[2] S. Weinberg, Phys. Rev. Lett. **110**, 261601 (2013).
[3] R.T. Kleiv, T.G. Steele, A. Zhang and I. Blokland, Phys. Rev. D **87**, 125018 (2013); D. Harnett, R.T. Kleiv, K. Moats and T.G. Steele, Nucl. Phys. A **850**, 110 (2011); J. Zhang, H.Y. Jin, Z.F. Zhang, T.G. Steele and D.H. Lu, Phys. Rev. D **79**, 114033 (2009); Fang Shi, T.G. Steele, V. Elias, K.B. Sprague, Ying Xue and A.H. Fariborz, Nucl. Phys. A **671**, 416 (2000); V. Elias, A.H. Fariborz, Fang Shi and T.G. Steele, Nucl. Phys. A **633**, 279 (1998).
[4] M. Wagner, et al., Acta Phys. Polon. Supp. **6** 847 (2013); C. Alexandrou, et al, JHEP **137**, 1304 (2013); T. Kunihiro, S. Muroya, A. Nakamura, C. Nonaka, M. Sekiguchi, H. Wada, in proceedings of *International IUPAP Conference on Few-Body Problems in Physics (FB 19), Bonn, Germany, 31 Aug - 5 Sep 2009*, EPJ Web Conf.3:03010 (2010); C. McNeile, in proceedings of *11th Int. Conf. on Meson-Nucleon Physics and the Structure of the Nucleon*, 10-14 Sept. 2007, Jülich, Germany; C. McNeile and C. Michael (UKQCD Collaboration), Phys. Rev. D **74**, 014508 (2006); N. Mathur et al, hep-ph/0607110; A. Hart et al (UKQCD Collaboration), Phys. Rev. D **74**, 114504 (2006); H. Wada (SCALAR Collaboration), Nucl. Phys. Proc. Suppl. **129**, 432 (2004); T. Kunihiro et al (SCALAR Collaboration), Phys. Rev. D **70**, 034504 (2003); N. Ishii, H. Suganuma and H. Matsufuru, Phys. Rev. D **66**, 014507 (2002); Xi-Yan Fang, Ping Hui, Qi-Zhou Chen and D. Schutte, Phys. Rev. D **65**, 114505 (2002); M.G. Alford and R.L. Jaffe, Nucl. Phys. B **578**, 367 (2000); C.J. Morningstar and M. Peardon, Phys. Rev. D **60**, 034509 (1999); J. Sexton, A. Vaccarino and D. Weingarten, Phy. Rev. Lett. **75**, 4563 (1995); G. Bali et al., Phys. Lett. B **309**, 378 (1993).
[5] I. Eshraim, S. Janowski, F. Giacosa and D.H. Rischke, Phys. Rev. D **87**, 054036 (2013); F. Giacosa, Phys. Rev. D **74**, 014028 (2006).
[6] J.R. Pelaez, PoS CD12, 047 (2013); R. Garcia-Martin, R. Kaminski, J.R. Pelaez, J. Ruiz de Elvira Phys. Rev. Lett. **107**, 072001 (2011); J.R. Pelaez, Phys. Rev. Lett. **97**, 242002 (2006).
[7] A.H. Fariborz, R. Jora, J. Schechter and M.N. Shahid, Phys. Rev. D **83**, 034018 (2011).
[8] A.H. Fariborz, R. Jora, J. Schechter and M.N. Shahid, Phys. Rev. D **84**, 094024 (2011); arXiv:1108.3581 [hep-ph].
[9] D. Black, A.H. Fariborz, R. Jora, N.W. Park, J. Schechter and M.N. Shahid, Mod. Phys. Lett. A **24**, 2285 (2009).
[10] A.H. Fariborz, N.W. Park, J. Schechter and M.N. Shahid, Phys. Rev. D **80**, 113001 (2009).
[11] D. Black, A.H. Fariborz, R. Jora, N.W. Park, J. Schechter and M.N. Shahid, Mod. Phys. Lett. A **28**, 2285 (2009).
[12] G. 't Hooft, G. Isidori, L. Maiani, A.D. Polosa anf V. Riquer, arXiv: 0801.2288 [hep-ph].
[13] A.H. Fariborz, R. Jora and J. Schechter, Phys. Rev. D **77**, 034006 (2008).
[14] A.H. Fariborz, R. Jora and J. Schechter, Phys. Rev. D **77**, 094004 (2008).
[15] L. Maiani, F. Piccinini, A.D. Polosa, V. Riquer, Eur. Phys. J. C **50**, 609 (2007); hep-ph/0604018.
[16] A.H. Fariborz, R. Jora and J. Schechter, Phys. Rev. D **76**, 014011 (2007).
[17] A.H. Fariborz, R. Jora and J. Schechter, Phys. Rev. D **76**, 114001 (2007).
[18] S. Narison, Phys. Rev. D **73**, 114024 (2006).
[19] H.Y. Cheng, C.K. Chua and K.C. Yang, Phys. Rev. D **73**, 014017 (2006).
[20] Yu. Kalashnikova, A. Kudryavtsev, A.V. Nefediev, J. Haidenbauer and C. Hanhart, Phys. Rev. C **73**, 045203 (2006).
[21] E. van Beveren, J. Costa, F. Kleefeld and G. Rupp, Phys. Rev. D **74**, 037501 (2006).
[22] M. Ablikim et al, Phys. Lett. B **633**, 681 (2006).
[23] N.A. Törnqvist, hep-ph/0606041.
[24] I. Caprini, G. Colangelo and H. Leutwyler, Phys. Rev. Lett. **96** (2006).
[25] F.J. Yndurain, Phys. Lett. B **578**, 99 (2004); Phys. Lett. B **612**, 245 (2005).
[26] T. Teshima, I. Kitamura and N. Morisita, Nucl. Phys. A **759**, 131 (2005).
[27] F. Giacosa, T. Gutsche, A. Faessler, Phys. Rev. C **71**, 025202 (2005).
[28] J. Vijande, A. Valcarce, F. Fernandez, B. Silvestre-Brac, Phys. Rev. D **72**, 034025 (2005).
[29] T.V. Brito, F.S. Navarra, M. Nielsen, M.E. Bracco, Phys. Lett. B **608**, 69 (2005).
[30] F. Giacosa, Th. Gutsche, V.E. Lyubovitskij, A. Faessler, Phys. Lett. B **622**, 277 (2005)
[31] A.H. Fariborz, R. Jora and J. Schechter, Phys. Rev. D **72**, 034001 (2005).
[32] A.H. Fariborz, R. Jora and J. Schechter, Int. J. of Mod. Phys. A **20**, 6178 (2005).
[33] T. Kunihiro, S. Muroya, A. Nakamura, C. Nonaka, M. Sekiguchi and H. Wada, Phys. Rev. D **70**, 034504 (2004).
[34] T. Umekawa, K. Naito, M. Oka and M. Takizawa, Phys. Rev. C **70**, 055205 (2004).
[35] L. Maiani, F. Piccinini, A.D. Polosa and V. Riquer, Phys. Rev. Lett. **93**, 212002 (2004).
[36] T. Teshima, I. Kitamura and N. Morisita, J. Phys. G. **30**, 663 (2004).
[37] M. Napsuciale and S. Rodriguez, Phys. Rev. D **70**, 094043 (2004).
[38] J.R. Pelaez, Phys. Rev. Lett. **92**, 102001 (2004).
[39] A. Ananthanarayan, I. Caprini, G. Colangelo, J. Gasser and H. Leutwyler, Phys. Lett. B **602**, 218 (2004).
.

[40] E.M. Aitala et al, Phys. Rev. Lett. **89**, 121801 (2002).
[41] G. Colangelo, J. Gasser and H. Leutwyler, Nucl. Phys. B **603**, 125 (2001).
[42] D. Black, A.H. Fariborz and J. Schechter, Phys. Rev. D **61**, 074030 (2000).
[43] D. Black, A.H. Fariborz, F. Sannino and J. Schechter, Phys. Rev. D **59**, 074026 (1999).
[44] D. Black, A.H. Fariborz, F. Sannino and J. Schechter, Phys. Rev. D **58**, 054012 (1998).
[45] D. Black, M. Harada and J. Shechter, Phys. Rev. Lett. **88**, 181603 (2002).
[46] The CLEO collaboration, Phys. Rev. D **61**, 012002 (2000).
[47] S. Teige et al, Phys. Rev. D **59**, 012001 (1999).
[48] M. Albaladejo and J.A. Oller, Phys. Rev. D **86**, 034003 (2012); J.A. Oller, E. Oset and J.R. Pelaez, Phys. Rev. D **59**, 074001 (1999).
[49] N.N. Achasov, Phys. Usp. **41**, 1149 (1999), hep-ph/9904223; N.N. Achasov and G.N. Shestakov, hep-ph/9904254.
[50] K. Igi and K. Hikasa, Phys. Rev. **D59**, 034005 (1999).
[51] J.A. Oller, E. Oset and J.R. Pelaez, Phys. Rev. Lett. **80**, 3452 (1998).
[52] S. Ishida, M. Ishida, T. Ishida, K. Takamatsu and T. Tsuru, Prog. Theor. Phys. **98**, 621 (1997). See also M. Ishida and S. Ishida, Talk given at 7th International Conference on Hadron Spectroscopy (Hadron 97), Upton, NY, 25-30 Aug. 1997, hep-ph/9712231.
[53] A.V. Anisovich and A.V. Sarantsev, Phys. Lett. **B413**, 137 (1997).
[54] S. Ishida, M.Y. Ishida, H. Takahashi, T. Ishida, K. Takamatsu and T Tsuru, Prog. Theor. Phys. **95**, 745 (1996).
[55] N.A. Törnqvist and M. Roos, Phys. Rev. Lett. **76**, 1575 (1996).
[56] M. Svec, Phys. Rev. **D53**, 2343 (1996).
[57] M. Harada, F. Sannino and J. Schechter, Phys. Rev. **D54**, 1991 (1996).
[58] N.A. Törnqvist, Z. Phys. C **68**, 647 (1995).
[59] F. Sannino and J. Schechter, Phys. Rev. **D52**, 96 (1995).
[60] G. Janssen, B.C. Pearce, K. Holinde and J. Speth, Phys. Rev. **D52**, 2690 (1995).
[61] R. Delbourgo and M.D. Scadron, Mod. Phys. Lett. **A10**, 251 (1995).
[62] N.N. Achasov and G.N. Shestakov, Phys. Rev. **D49**, 5779 (1994). A summary of the recent work of the Novosibirsk group is given in N.N. Achasov, arXiv:0810.2601[hep-ph].
[63] R. Kamínski, L. Leśniak and J. P. Maillet, Phys. Rev. **D50**, 3145 (1994).
[64] N.N. Achasov and G.N. Shestakov, Phys. Rev. D **49**, 5779 (1994).
[65] D. Morgan and M. Pennington, Phys. Rev. **D48**, 1185 (1993).
[66] A.A. Bolokhov, A.N. Manashov, M.V. Polyakov and V.V. Vereshagin, Phys. Rev. **D48**, 3090 (1993).
[67] J. Weinstein and N. Isgur, Phys. Rev. D **41**, 2236 (1990).
[68] D. Aston et al., Nucl. Phys. B **296**, 493 (1988).
[69] E. van Beveren, T.A. Rijken, K. Metzger, C. Dullemond, G. Rupp and J.E. Ribeiro, Z. Phys. C **30**, 615 (1986).
[70] E. van Beveren, T.A. Rijken, K. Metzger, C. Dullemond, G. Rupp and J.E. Ribeiro, Z. Phys. **C30**, 615 (1986).
[71] R.L. Jaffe, Phys. Rev. D **15**, 267 (1977).
[72] A.H. Fariborz, Phys. Rev. D **74**, 054030 (2006).
[73] M. Napsuciale and S. Rodriguez, Phys. Rev. D **70**, 094043 (2004).
[74] A.H. Fariborz, Int. J. of Mod. Phys. A **19**, 2095 (2004).
[75] A.H. Fariborz, Int. J. of Mod. Phys. A **19**, 5417 (2004).
[76] T. Teshima, I. Kitamura and N. Morisita, J. Phys. G **28**, 1391 (2002); *ibid* **30**, 663 (2004).
[77] F. Close and N. Tornqvist, *ibid.* **28**, R249 (2002).
[78] D. Black, A.H. Fariborz and J. Schechter, Phys. Rev. D **61**, 074001 (2000).
[79] A.H. Fariborz, R. Jora and J. Schechter, Phys. Rev. D **79**, 074014 (2009).
[80] E. Klempt and A. Zaitsev, Phys. Rept. **454**,1 (2007); arXiv:0708.4016v1.
[81] M. Albaladejo, J.A. Oller and L. Roca, Phys. Rev. **D** 82, 094019 (2010).
[82] S. Weinberg, Physica A **96**, 327 (1979); J. Gasser and H. Leutwyler, Annalas Phys. **158**, 142 (1984); Nucl. Phys. B **250**, 465 (1985).
[83] J. Bijnens, in proceedings of the 2nd International PrimeNet Workshop, Forschungszentrum Juelich, Germany, 26-28 (2011). CNUM: C11-09-26.8, arXiv:1110.6004 [hep-ph].
[84] R. Escribano, P. Masjuan, J.J. Sanz-Cillero, JHEP 1105, 094 (2011).
[85] V. Dorofeev et al, Phys. Lett. B **651**, 22 (2007).
[86] A.M. Blik et al, Phys. Atom Nucl. **72**, 231 (2009).
[87] M. Amaryan et al, "Decays of Light Mesons in CLAS," in proceedings of the second International PrimeNet Workshop, September 26-28, 2011, Jülich, Germany, p. 80-82; arXiv: 1204.5509 [nucl-ex].
[88] B.R. Jany, in proceedings of Symposium on Meson Physics at COSY-11 and WASA-at-COSY, Cracow, Poland, June 17-22, 2007 [AIP Conf. Proc. **950**, 209 (2007)].
WASA-at-COSY Collaboration, B.R. Jany et al, in proceedings of MENU 2007, the 11th International Conference on Meson-Nucleon Physics and the Structure of the Nucleon, September 10-14, 2007, Jülich, Germany [SLAC eConf **C070910**, 169 (2007)].
M. Büscher, in proceedings of *Workshop on Scalar Mesons and Related Topics*, February 11-16, 2008, Lisbon, Portugal [AIP Conf. Proc. **1030**, 40 (2008)].
[89] D. Black, A.H. Fariborz, S. Moussa, S. Nasri and J. Schechter, Phys. Rev. D **64**, 014031 (2001).
[90] A.H. Fariborz, Int. J. Mod. Phys. A **26**, 2327 (2011).

[91] A.H. Fariborz and J. Schechter, Phys. Rev. D **60**, 034002 (1999).
[92] A.H. Fariborz, R. Jora, J. Schechter and M.N. Shahid, Phys. Rev. D **84**, 113004 (2011); arXiv:1106.4538 [hep-ph].
[93] A.H. Fariborz, E. Pourjafarabadi, J. Schechter and M. Zebarjad, "Chiral nonet mixing in πK scattering," in preperation.
[94] A.H. Fariborz, E. Pourjafarabadi, J. Schechter, S. Zarepour and M. Zebarjad, "Chiral nonet mixing in $\pi\eta$ scattering," in preperation.
[95] A.H. Fariborz, E. Pourjafarabadi, J. Schechter, S. Zarepour and M. Zebarjad, "Effect of higher order $U(1)_A$ breaking on eta systems," in preperation.
[96] The isospin violation case for the single-M linear sigma model was treated in J. Schechter and Y. Ueda, Phys. Rev. D **4**, 733 (1971).
[97] A. Abdel-Rehim, D. Black, A.H. Fariborz and J. Schechter, Phys. Rev. D **67**, 054001 (2003).
[98] Various unitarization schemes are contrasted in Zhi-Hui Guo, L.Y. Xiao and H.Q. Zheng, Int. J .Mod. Phys. A **22**, 4603 (2007).